

Markerless Multi-view 3D Human Pose Estimation: a survey

Ana Filipa Rodrigues Nogueira^{a,b,*}, Hélder P. Oliveira^{a,c} and Luís F. Teixeira^{a,b}

^aInstituto de Engenharia de Sistemas e Computadores, Tecnologia e Ciência (INESC TEC), Rua Dr. Roberto Frias, 4200-465, Porto, Portugal

^bFaculdade de Engenharia da Universidade do Porto (FEUP), Rua Dr. Roberto Frias, 4200-465, Porto, Portugal

^cFaculdade de Ciências da Universidade do Porto (FCUP), Rua do Campo Alegre, 1021-1055, Porto, Portugal

ARTICLE INFO

Keywords:

3D Human Pose Estimation
Multi-view
Supervision level
Temporal consistency
Multi-modal

ABSTRACT

3D human pose estimation aims to reconstruct the human skeleton of all the individuals in a scene by detecting several body joints. The creation of accurate and efficient methods is required for several real-world applications including animation, human-robot interaction, surveillance systems or sports, among many others. However, several obstacles such as occlusions, random camera perspectives, or the scarcity of 3D labelled data, have been hampering the models' performance and limiting their deployment in real-world scenarios. The higher availability of cameras has led researchers to explore multi-view solutions due to the advantage of being able to exploit different perspectives to reconstruct the pose.

Thus, the goal of this survey is to present an overview of the methodologies used to estimate the 3D pose in multi-view settings, understand what were the strategies found to address the various challenges and also, identify their limitations. Based on the reviewed articles, it was possible to find that no method is yet capable of solving all the challenges associated with the reconstruction of the 3D pose. Due to the existing trade-off between complexity and performance, the best method depends on the application scenario. Therefore, further research is still required to develop an approach capable of quickly inferring a highly accurate 3D pose with bearable computation cost. To this goal, techniques such as active learning, methods that learn with a low level of supervision, the incorporation of temporal consistency, view selection, estimation of depth information and multi-modal approaches might be interesting strategies to keep in mind when developing a new methodology to solve this task.

1. Introduction

3D human pose estimation aims to reconstruct the body configuration of all persons in a scene. Finding solutions for this task is essential for numerous applications ranging from human-robot interaction [92], animation [37], gaming, action recognition [53], rehabilitation assessments, surveillance systems [23], sports [60, 9], live broadcasts [28], human-computer interaction, such as recognising sign language [25], among many others. As an example of application, the work of Mustafa et al. [60] showed that the reconstruction of the 3D pose in a multi-view setting helped the creation of a method for 4D dynamic scene understanding with numerous interacting individuals, such as sports games.

Therefore, it is necessary to develop solutions that can solve this task effectively and efficiently, without the need to use markers. Because the use of markers imposes many restrictions on the application scenarios in which the methods can be used. Furthermore, placing markers over clothing can lead to incorrect readings of the person's keypoints due to possible displacement of a marker during the performance of movements [74].

Methods for estimating the 2D pose have been widely explored, however, those only allowed the reconstruction of a surface pose. Thus, to capture the volume of the body of the person, it is necessary to determine the 3D pose.

Nonetheless, since there have been more advances in 2D pose estimation methods, many 3D estimation algorithms, use the 2D pose estimations for each view to reconstruct the 3D pose.

The use of multiple views helps to capture the whole body geometry making it easier and more suitable for 3D pose estimation than monocular methodologies [81]. However, the occurrence of occlusions, poor camera calibration, lack of 3D annotated data, similarities or variations in human appearance, and difficulties in associating the multiple views and generalise to new perspectives are some challenges methods developed for multi-view systems have to overcome to accurately estimate the 3D pose [9, 88].

1.1. Previous literature reviews

Solutions to accurately and efficiently estimate the 3D human pose have been widely explored over the years. Thus, there are numerous surveys summarizing and evaluating most of the existing works.

Initially, most of the methodologies were developed for single-view inputs. Therefore, there are several surveys addressing 3D pose estimation based on monocular images [17, 76, 57, 41, 54, 51]. The main findings are that, even though deep learning has brought considerable improvements to the estimation of the 3D pose, occlusions, crowded scenarios, and a lack of datasets that can realistically mimic real-world settings still limit the models' performance and restrain their real-world employment. For future research, it is suggested the use of transfer learning [57], synthetic data [57, 54], models with little supervision [54], or complementary information by, for example, exploiting a multi-modal approach [76, 54], incorporate global and local context to

*Corresponding author

✉ ana.f.rodrigues@inesctec.pt (A.F.R. Nogueira);

helder.f.oliveira@inesctec.pt (H.P. Oliveira); luisft@fe.up.pt (L.F. Teixeira)

ORCID(s): 0000-0002-9413-3300 (A.F.R. Nogueira);

0000-0002-6193-8540 (H.P. Oliveira); 0000-0002-4050-7880 (L.F. Teixeira)

obtain more distinguishing characteristics [17], explore the interactions between the individuals and the scene or the objects [41, 54, 51] or add the use of temporal information [57]. In addition, multi-view geometry is pointed out as a solution for data scarcity and the ambiguities in monocular 3D pose estimation [41, 54, 51].

The increased availability of multi-camera setups has prompted further research on the benefits of having various camera perspectives. As a result, several surveys, besides analysing single-view methods, also cover multi-view approaches [96, 55, 22, 70, 85, 62, 8, 100, 49, 47]. The literature review of Holte et al. [34] is the only one found, solely dedicated to multi-view methodologies. According to the analysed surveys, most of the problems observed in monocular settings are the same for multi-view, namely, the lack of annotated in-the-wild datasets or with rare poses [55, 70, 8, 22, 49, 85, 100, 62], the difficulty in identifying the several poses in crowded scenarios, and the occlusions [96, 47, 100, 49, 34]. Even though, overcoming the occlusions problem benefits from the different view perspectives, it still remains a challenge in some situations. Besides, the increase in the number of viewpoints leads to the need for more complex models to be able to deal with the information acquired from all perspectives. This translates into slower inference runtime, forcing a balance between complexity and speed [8, 47, 100, 49]. Furthermore, the bad image quality in terms of focus or blur [100, 47, 49, 34], the inaccuracies of 2D pose estimations which affect the models that use 2D-3D lifting [49, 34] are also, factors negatively influencing the quality of the predictions. So, there are still a lot of opportunities for improvement, such as considering the human interactions either with other humans or the surrounding environment [70, 85, 100, 34], the increase of the generality in order for the same method to be suitable across multiple applications and independent of the presented viewpoints [47, 49, 34]. Also, several surveys recommend the use of neural architecture search for a better and more efficient design of neural networks [85, 47, 100, 49], taking advantage of temporal information, even the adaptation of methods from monocular to multi-view [47, 22], the use of transfer learning [55] and data augmentation [100]. Finally, to combat the scarcity of annotated datasets, several strategies are suggested like using unsupervised, semi-supervised or weakly-supervised models [55, 85], or the use of active learning to alleviate the human workload [62].

Moreover, some surveys briefly mention multi-modal approaches, mainly, combining vision and Inertial Measurement Units (IMUs) sensors but also, depth sensors, point clouds or Radio-Frequency (RF), which allow to obtain more accurate estimations, demonstrating the benefits of having complementary information [22, 100, 49].

Therefore, the scope of the present survey is in markerless methods, so, it is only going to be considered methods that do not require people to have attached sensors. Also, the literature lacks a review focus on methods which used various cameras to determine the pose. Most of the surveys that address these methods only present a relatively brief

section, as can be seen in Table 1. Thus, this literature review will solely focus on 3D Human Pose Estimation based on data from multiple cameras and also, acknowledge works that use different types of sensors, such as Red Green Blue-Depth (RGB-D) cameras, Time-of-Flight (ToF) cameras or wireless devices, to obtain the 3D pose in a multi-view environment.

1.2. Search Process

The research process, Figure 1, was conducted in September 2023 and updated in June 2024, using the search engine for scientific articles: Scopus. Several combinations of the following keywords were used: 3D pose estimation; multi-view/multi-camera; Channel State Information (CSI), RF, Wi-Fi, multi-sensor, multi-modal, Light Detection And Ranging (LiDAR); data-efficiency techniques.

This search process resulted in 204 works, and the following criteria were then applied to filter the results:

1. Remove duplicates
2. Exclude the articles that are entirely unrelated to the subject by analysing the title and abstract.
3. Include only peer-reviewed works written in English.
4. Analyse the body of the text and include only the relevant works to the study at hand.

After applying the above criteria, it resulted in 73 works that were fully revised and used to construct this literature review. In Figure 2 is possible to see the growing interest in this area.

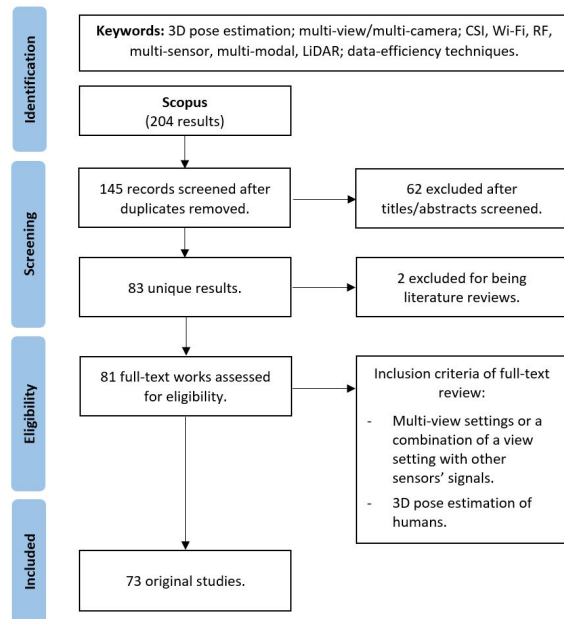


Figure 1: PRISMA diagram of the conducted research process (adapted from [63]).

The rest of this literature review is organised in the following way: Chapter 2 - Datasets, Chapter 3 - Evaluation Metrics, Chapter 4 - Multi-view approaches, Chapter 5 - Multi-modal approaches, Chapter 6 - Conclusion.

Table 1

Table of a comparative analysis between the surveys on 3D pose estimation

Papers	Year	Monocular view methods	Multi-view methods	Wi-Fi, RF or other sensors	Datasets	Benchmarking Performance	Metrics
Human pose estimation and activity recognition from multi-view videos: Comparative explorations of recent developments [34]	2012	✗	✓ (24 works)	✗	✓	✓	✗
A survey of human pose estimation: The body parts parsing based methods [55]	2015	✓	✓ (6 works)	✗	✓	✓	✗
3D Human pose estimation: A review of the literature and analysis of covariates [70]	2016	✓	✓ (11 works)	✗	✓	✓	✓
A survey on monocular 3D human pose estimation [41]	2020	✓	✗	✗	✓	✓	✓
Monocular human pose estimation: A survey of deep learning-based methods [17]	2020	✓	✗	✗	✓	✓	✓
Deep 3D human pose estimation: A review [85]	2021	✓	✓ (16 works)	✗	✓	✓	✓
Deep Learning Methods for 3D Human Pose Estimation under Different Supervision Paradigms: A Survey [96]	2021	✓	✓ (11 works)	✗	✓	✓	✓
A review of 3D human pose estimation algorithms for markerless motion capture [22]	2021	✓	✓ (7 works)	✗	✓	✓	✓
Human pose estimation and its application to action recognition: A survey [76]	2021	✓	✗	✗	✓	✓	✗
A review of deep learning techniques for 2D and 3D human pose estimation [8]	2021	✓	✓ (9 works)	✗	✓	✓	✓
A Survey of Recent Advances on Two-Step 3D Human Pose Estimation [57]	2022	✓	✗	✗	✓	✓	✗
Human pose estimation using deep learning: review, methodologies, progress and future research directions [47]	2022	✓	✓ (9 works)	✗	✓	✗	✓
Recent Advances of Monocular 2D and 3D Human Pose Estimation: A Deep Learning Perspective [54]	2022	✓	✗	✗	✓	✓	✓
Deep Learning-Based Human Pose Estimation: A Survey [100]	2023	✓	✓ (26 works)	✓	✓	✓	✓
Efficient Annotation and Learning for 3D Hand Pose Estimation: A Survey [62]	2023	✓	✓ (19 works)	✗	✗	✗	✗
Overview of 3D Human Pose Estimation [51]	2023	✓	✓ (17 works)	✗	✓	✓	✓
Vision-Based Human Pose Estimation via Deep Learning: A Survey [49]	2023	✓	✓ (8 works)	✓	✓	✓	✓
Markerless Multi-view 3D Human Pose Estimation: a survey (Ours)	2024	✗	✓ (57 works)	✓	✓	✓	✓

2. Datasets

The most used datasets to train and assess the performance of 3D Human Pose Estimation in multi-view settings are Human3.6M [39], Campus [5], Shelf [5] and CMU Panoptic [43].

Human3.6M [39] is a commonly used dataset for estimating the 3D pose of a single person. The data was collected in a laboratory with 4 digital video cameras positioned in the corners, 1 ToF on top of one digital camera, and 10 motion cameras spread throughout the walls, with 4 on each side and 2 in the middle of the horizontal edge. The data

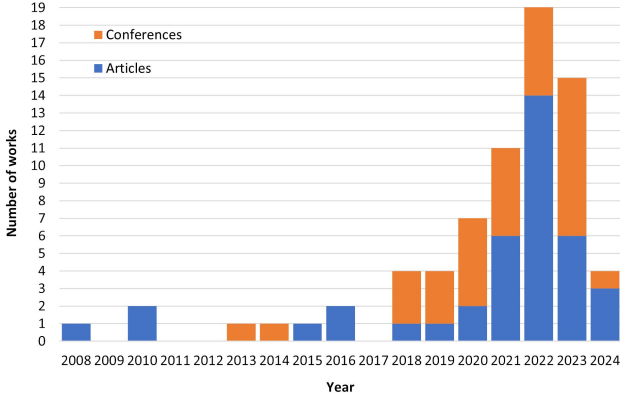


Figure 2: Evolution of the published works found in Scopus database for markerless 3D pose estimation in multi-camera settings or by using other types of sensors such as RGB-D cameras, ToF cameras or wireless sensors.

included 15 distinct actions: discussion, greeting, posing, walking, eating, sitting and taking photographs, among others. These actions were enacted by a total of 11 unique individuals, encompassing both male and female participants. Out of these 11 individuals, two males and two females were exclusively included in the testing set.

Campus [5] consists of three persons interacting and being recorded by three cameras in an outdoor environment. Annotations for the body joints of the three individuals were created for cameras 1 and 2. Subsequently, these annotations were triangulated and projected to generate the annotations for the third perspective.

Shelf [5] comprises four people disassembling a shelf in an indoor setting which is being recorded by five cameras. Due to the consistent occlusion of one participant (Actor 4) in the majority of the frames, the pose estimation corresponding to that person is usually disregarded during the evaluation. The 3D ground-truth annotations were generated by triangulating the body joint annotations from the 2nd, 3rd, and 4th camera perspectives.

CMU Panoptic [43] is the dataset with the greatest number of perspectives available, providing a total of 521 views (480 VGA, 31 HD and 10 Kinetic cameras). The data was acquired in a controlled environment and includes both actions performed in groups and individually. Participants were organised into groups of a maximum of 8 elements to participate in social activities such as games like Ultimatum or Haggling, group discussions, musical performances, or dancing.

Other datasets were captured with a specific application scenario in mind, such as KTH Multiview Football [46, 45], which allows tracking people on a football field, or MPII Cooking [69], to track people during their cooking process. Table 2 summarises the existing datasets and their main characteristics. Table 3, Table 4 and Appendix A present the benchmarking for the several datasets used in the revised works.

3. Evaluation Metrics

This section presents the evaluation metrics specific to human pose estimation. The most widely used metrics to evaluate the quality of the 3D pose estimations are Percentage of Correct Parts (PCP), Mean Per Joint Position Error (MPJPE), Percentage of Correct Keypoints (PCK), or Average Precision (AP). Nonetheless, other less frequently used metrics like Mean Average Precision (mAP), Area Under the Curve (AUC), Mean Per Joint Angle Error (MP-JAE) and Mean of the Root Position Error (MRPE) are also introduced.

PCP determines the limb detection accuracy. A limb is considered correct if the distance between the predicted limb ends and the ground-truth limb joint locations is less or equal to a certain value α of the limb's length, (see Eq. 1).

$$\frac{\|s_p - s'_p\| + \|e_p - e'_p\|}{2} \leq \alpha \|s_p - e_p\| \quad (1)$$

s_p and e_p are the 3D ground-truth coordinates of the beginning and ending points of the body part p .

s'_p and e'_p are the corresponding estimated coordinates of the beginning and ending points of the body part p .

α is the threshold, normally defined as 0.5.

MPJPE, also known as 3D error, corresponds to the average Euclidean distance between the estimated joints and the respective true joint location, (see Eq. 2).

$$\text{MPJPE}(S) = \frac{1}{N_S} \sum_{i=1}^{N_S} \|G_i - P_i\|_2 \quad (2)$$

G_i is the ground-truth position of the i -the joint.

P_i is the predicted position of the i -the joint.

N_S is the number of joints of the S skeleton.

Some researchers also report results using a variant of MPJPE, Procrustes Alignment MPJPE (PA-MPJPE), which uses Procrustes alignment [32] on the ground-truth and estimate joints before calculating MPJPE.

PCK consists in the % of points in which the distance between the estimated and the real value is inferior to a defined threshold, (see Eq. 3).

$$\text{PCK}_{k_i} = \frac{1}{N} \sum_{i=1}^N \delta \left(\left\| P_k^i - G_k^i \right\|_2 \leq t_j \right) \quad (3)$$

PCK_{k_i} is the PCK value of the i -the keypoint of the k -the skeleton.

t_j is the j -the defined threshold.

P_k^i and G_k^i represent the coordinates of the i -the joint of the k -the predicted skeleton and the ground truth of that joint, respectively.

$$\delta(\cdot) = \begin{cases} 1 & \text{if } \left\| P_k^i - G_k^i \right\|_2 \leq t_j \text{ is True} \\ 0 & \text{otherwise} \end{cases}$$

Table 2

Summary of the found datasets for Multi-view 3D Human Pose Estimation.

Datasets	Year	Size	N ^o cameras	N ^o subjects	Characteristics
HumanEva-I [74]	2010	40 060	7	4	Single-person dataset that includes 6 distinct actions: random hand movements, boxing, playing with a ball by tossing and catching, walking, running and a combined sequence in which the subject begins walking, then runs and at the end, balances on each foot alternately. The ground-truth data was obtained using a MoCap system with 6 cameras.
HumanEva-II [74]	2010	2 460	4	2	Single-person performing an extended sequence of actions compared to HumanEva-I. The ground-truth motion was captured using a MoCap system with 12 cameras. This is only a test set, the models are supposed to be trained and validated with the data from HumanEva-I.
Utrecht Multi-Person Motion (UMPM) [1]	2011	400 000	4	30	Consists of 9 different scenarios recorded with 1 to 4 people in the scene. Ground-truth was captured with 14 Vicon MoCap cameras.
KTH Multiview Football I [46]	2012	257	3	2	Professional football players during a match of the Allsvenskan league.
KTH Multiview Football II [45]	2013	800	3	2	Extended version of KTH Multiview Football I.
Human3.6M [39]	2014	3 600 000	4	11	Only single-person scenarios realizing one of the 17 pre-defined actions. People have IMU sensors attached for a better annotation of the keypoints.
Campus [5]	2014	2 000	3	3	Multiple people interacting in an outdoor environment.
Shelf [5]	2014	3 200	5	4	Multiple people in a room disassembling a shelf.
CMU Panoptic [43]	2015	1 500 000	521	1-8 per frame	Contains scenes with a single person doing a set of movements and scenarios with multiple people engaging in social activities. (521 cameras: 480 VGA camera; 31 HD cameras and 10 Kinect II Sensors).
MPII Cooking 2 [69]	2015	2 881 616	8	30	Single-person preparing several dishes.
NTU RGB+D [72]	2016	4 000 000	3	40	There are 60 different actions; some were performed with just one person in the scene and some required a multi-person setting. It was collected depth maps, RGB images and videos, 3D joint information, and infrared sequences.
MPI-INF-3DHP [59]	2017	>1 300 000	14	8	Single-person performing one of the 8 pre-defined activities.
Total Capture [80]	2017	1 892 176	8	5	Single-person either walking, acting, doing freestyle movements or a range of motion sequences. All frames have a multi-view video, IMU and Vicon labelling.
PKU-MMD [19]	2017	5 312 580	3	66	The subjects performed various actions by themselves and in group. Contains depth maps, RGB images, skeleton joints, infrared sequences, and RGB videos.
WILDTRACK [13]	2018	36 000	7	313	Data captured in the street in front of the ETH Zurich University's main building.
Multi-View Operating Room (MVOR) [78]	2018	732	3	10	Consists of images recorded during 4 days in an interventional room at the University Hospital of Strasbourg.
NTU RGB+D 120 [52]	2019	8 000 000	3	106	It is an extension of NTU RGB+D and it has 60 more different actions, making a total of 120 actions.

How2Sign [25]	2021	~7 503 218	3	11	Consists of people doing sign language. Besides images, it also, contains speech, English transcripts, gloss, pose information and depth information.
HuMoMM [97]	2023	262 000	5	18	Includes 30 different actions: 20 performed individually and 10 in group. Contains RGB images and depth images and also, provides multi-modal annotations that comprehend 2D and 3D keypoints, SMPL parameters and action categories.
PKUInfantV [95]	2024	~2 000 000	3	170	It comprises 510 videos recorded in a hospital setting, and the movements of the infant were categorized as either normal or abnormal writhing motions by a physician. This dataset led to the creation of two other datasets: one consisting of 15 924 annotated images obtained from 420 videos in the PKUInfantV dataset, and the other being a downsampled version featuring solely the segments of the videos in which the infant exhibited movement.

AP is calculated using MPIPE (see Eq. 2) as the thresholding metric between the ground truth and the predicted keypoints, (see Eq. 4). For example, AP@50 refers to the AP calculated considering a pose correctly estimated if the MPIPE < 50mm.

$$AP@k = \frac{1}{P} \sum_{p=1}^P \frac{TP_p}{TP_p + FP_p} \quad (4)$$

TP corresponds to True Positive.

FP corresponds to False Positive.

P is the number of people in the scene.

k is the threshold in mm.

mAP is the average value of all AP over all considered thresholds, (see Eq. 5).

$$mAP = \frac{1}{T} \sum_{k=1}^T AP@k \quad (5)$$

T is the number of considered thresholds.

AUC integrates the curve that evaluates the model performance across all PCK thresholds.

MPJAE measures the average, across all angles, of the absolute difference in degrees between the actual joint angles and the estimates, (see Eq. 6).

$$MPJAE = \frac{1}{N} \sum_{i=1}^N \left| (x_i - x'_i) \bmod \pm 180^\circ \right| \quad (6)$$

N is the total number of joints.

P_i is the estimated pose vector.

P'_i is the ground-truth pose vector.

mod is the modulus operator, the term mod $\pm 180^\circ$ applies to angles brings them into the range of $[-180^\circ, +180^\circ]$.

MRPE consists of the mean Euclidean distance between the predicted root localization and the ground-truth root localization, (see Eq. 7).

$$MRPE = \frac{1}{N} \sum_{i=1}^N \left\| R^{(i)'} - R^{(i)} \right\|_2 \quad (7)$$

$R^{(i)'}$ is the coordinates of the predicted root.

$R^{(i)}$ is the coordinates of the ground-truth root.

4. Multi-view approaches

The availability of multiple views, on the one hand, provides more information for constructing the 3D pose, on the other hand, introduces a new problem, which is how to associate these multiple views. [88]

Most of the earlier methodologies were developed to address this task in single-person scenarios, nonetheless, the majority of the more recent approaches focus on multi-person settings. Therefore, the existing methods can be divided into single-person (Section 4.1) or multi-person approaches (Section 4.2), according to the number of people in the scene.

4.1. Single-person approaches

In this section, it's presented methods developed to retrieve the 3D pose of scenarios with just one individual.

Sigal et al. [74] introduced the HumanEva datasets to combat the lack of datasets for multi-view 3D pose estimation and provide a benchmark so that developed methods could be compared fairly. Thus, to provide intuition on how to work with their dataset, a baseline model was proposed which consisted of a Bayesian filtering method whose parameters were optimised using Sequential Importance Resampling and Annealed Particle Filtering.

To try to create a method which provides a fast inference while still giving a good performance, Wang and Chung [88] employed a bottom-up approach by first, determining

all possible body part candidates for each view. Then, used a linear-combination expression to determine which detected parts had correspondence across all views, thus decreasing the number of erroneous candidates. Finally, a belief propagation process is applied to group all the parts into a 3D pose.

Mehrizi et al. [58] followed a two-stage approach. Thus, the researchers proposed a Deep Neural Network (DNN) composed of a perceptron network to determine the 2D poses and the hierarchical texture information for each view, and by a half-hourglass with skip connections which uses the mentioned information to infer the 3D pose. Showing the importance of sharing the texture information to improve the estimation of the 3D pose.

Amin et al. [2] for 3D single-person estimation, used the Pictorial Structures (PS) model to estimate the 2D poses and then, triangulation to recover the 3D pose. Although the employed method has demonstrated good performance on the HumanEva-I dataset, it's dependent on the camera setup to learn the pairwise appearance terms.

As for Remelli et al. [65], they presented an efficient method of reconstructing the pose without substantially increasing the computational cost. To do so, the authors introduced a faster version of the Direct Linear Transform method to lift the predicted 2D skeletons to 3D poses. The 2D poses are generated by exploring 3D geometry and camera projections.

Solichah et al. [75] applied the OpenPose [11] algorithm, which allows the implementation of a real-time keypoint detector for multi-persons on single images, to forecast the 2D poses. Then, used triangulation to achieve the final 3D pose. Although the method produced satisfactory results, it requires a proper calibration of the camera settings. The approach proposed by Kadkhodamohammadi and Padoy [44] uses the following pipeline: estimation of the 2D poses using a single-view detector, match of the 2D poses across views using epipolar geometry and regress the 3D pose using a multilayer neural network composed of multiple stages. The authors have shown that the inclusion of distinct perspectives enhances the model's performance. Nonetheless, one major drawback of their method is the high reliance on the camera calibration settings and the features of the single-view pose detector.

The study conducted by Wan et al. [82] seeks to improve the correlation of 2D keypoints across multiple views by employing a Multi-view Fusion module and to refine the 3D pose estimation through the utilisation of Holistic Triangulation with anatomy constraints. The Multi-view Fusion module integrates pseudo-heatmaps from various views, created based on detected keypoints in the reference view, with the initial heatmap to produce a more precise heatmap. Holistic triangulation with anatomy constraints is designed to simultaneously correlate all views through the integration of a re-projection term based on multi-view geometric constraints and a Principal Component Analysis (PCA) reconstruction term to enforce anatomical consistency. Despite its rather

good performance, the model encounters challenges in reconstructing poses for unseen movements and lacks adaptability to systems featuring a different number of cameras than those used during training.

As evidenced by previously revised methods, numerous methodologies rely on a fixed camera setup and are unable to generalise to new perspectives. To overcome this issue, Bartol et al. [4] suggested a triangulation method based on stochasticity. Which after generating the 2D poses for each view, randomly chooses a subgroup of views and combines the corresponding 2D poses through triangulation to produce the 3D pose. This second step is repeated several times to create various hypotheses, to which a score is assigned to allow the computation of the weighted average of all hypotheses and consequently, choose the most appropriate hypothesis. Jiang et al. [42] have proposed a method, called Probabilistic Triangulation, that approximates the camera pose distribution. The parameters of this distribution are initialised using 2D heatmaps estimated from the input RGB images and are then continuously updated using Monte Carlo sampling. This approach reduces the reliance on calibration parameters, making it possible to estimate the 3D pose in uncalibrated settings. Nonetheless, it still requires the model to be trained with calibrated data.

Nakatsuka and Komorita [61] developed a method to obtain robust 3D pose estimations in demanding environments with limited views and low-resolution data. In this type of environment, the occurrence of occlusions and the lack of visual information are very frequent, damaging the prediction of the pose, to overcome this challenge some researchers have used temporal consistency. Nonetheless, Nakatsuka and Komorita argue that imposing temporal consistency may suppress abrupt and tiny changes which might hinder the overall model's performance. Thereby, they proposed a method composed of two components: one for regressing the 3D pose using images as input, and the other for refining the previous 3D pose estimation, utilising a gated temporal convolution network to correct just the keypoints predicted with poor confidence. The authors claim that their approach could be further optimised by employing a lightweight 3D pose estimator.

Xia and Zhang introduced VitPose [89], a model composed of a CNN backbone used to capture the low-level features; the encoder part of the Vision Transformer to capture the long-range relationship between the human body joints in one perspective and their association with the joints in another perspective; and the Simple Feature Fusion Network, which allows to weightily fuse views to prevent views that give poor pose predictions from harming model performance. Hence, this method provided a more robust fusion step and also, showed that the exploration of long-distance relationships enables more exact 2D pose estimations. Cai et al. [10] also explored the fusion of features. However, the researchers focus on fusing features from multiple frames with those from various perspectives. To achieve this, a transformer encoder is used to create a global feature that combines all the features from different views

and frames. Then, a transformer decoder is used to fuse the global features with the features specific from each view, yielding a more meaningful set of features to estimate the 3D pose. The employment of this fusion scheme proved to be effective in mitigating the depth uncertainty impact, in addition to demonstrating the potential of methodologies that do not require prior knowledge of camera parameters.

The computational load imposed by Convolutional Neural Network (CNN)-based models may limit their application in real-world scenarios. To surpass this problem, Hwang et al. [36] designed a system consisting of several edge devices and a central server. In which each edge device was responsible for estimating the 2D pose of the received image using a CNN and then, sending it along with the respective timestamp to the central server. The central server, in turn, triangulates using Direct Linear Transform (DLT) the received 2D poses that were detected at roughly the same time to produce the 3D pose. Hence, this system distributes the computational burden of the CNN among edge devices and also reduces data traffic by transmitting only the 2D poses and timestamps rather than RGB images, making it more suitable for real-time applications in the real-world.

4.1.1. Methods under different supervision levels

The scarcity of labelled datasets significantly restricts the models' outcomes. Therefore, unsupervised, weakly-supervised, semi-supervised and self-supervised methods have been proposed to combat the dependence on 3D labelled datasets.

An example is the work of Rhodin et al. [67] which employed a semi-supervised method capable of learning from unlabelled images, a geometry-aware representation of the human body. Then, used some supervision to learn the mapping from the 3D geometry representation to the 3D pose. Inspired by this methodology, Kundu et al. [48] introduced an unsupervised method that uses a geometry-aware bottleneck to generate a comprehensible latent space for representing the 3D poses. Rochette et al. [68], on the other hand, explored a weakly-supervised method which uses a multi-view consistency loss and a re-projection consistency loss to determine the 3D pose using only one image. Similarly, Ma et al. [56] also proposed a self-supervised approach in which the loss function leverages information from more than one view to completely disentangle the camera perspective from the 3D human body skeleton and consequently, surpass the projection ambiguity issue observed in a monocular setting. During their research, the authors concluded that the use of more views throughout the training process would further boost the performance of their network.

In the research work carried out by Zhao et al. [99], a new loss function, Triangulation Residual Loss, has been proposed, whose objective is to minimise the total distances between view rays and 3D pose estimation retrieved through triangulation. This novel loss function aims to enforce multi-view geometric consistency, facilitating the efficient self-supervised training of the model. As for Jenni and Favaro

[40], they proposed a pre-training technique using self-supervised learning, to determine the synchronisation between two images and whether one image is inverted horizontally in relation to the other, with the objective of learning a meaningful representation suitable to be used by a network to estimate the 3D pose. Also, the authors suggest removing the background for static images to prevent irrelevant features from being learnt during the self-supervised learning task. In addition, Liu et al. [53] also, introduced a method which relies only on two views to reconstruct the pose, without requiring to know any camera configurations. So, their method after extracting the 2D poses of each image, used a self-supervised 3D regression network able to produce virtual views using orthogonal projections of the human body, allowing the model to thoroughly understand the human body spatial structure and the transformations necessary to project one perspective onto another. Concerning the work of Yin et al. [95], a self-supervised method incorporating temporal convolution blocks and spatio-temporal attention mechanisms has been investigated. The methodology employed involved the exploration of re-projection and view consistency methods, which enabled an accurate retrieval of the 3D pose of infants without the need for 3D labels or definition of camera calibration parameters.

In contrast with the previous works, Feng et al. [29] proposed a method to enhance the data labelling process instead of trying to learn from the available unlabelled data or producing new synthetic data. Feng et al. have used an Active learning-based methodology (see Figure 3) to efficiently annotate the data without considerably increasing the overall computational cost. Moreover, the researchers have shown that this strategy employed whether alone or in conjunction with self-training can boost the labelling of the data and consequently, enhance the overall 3D pose estimation outcomes.

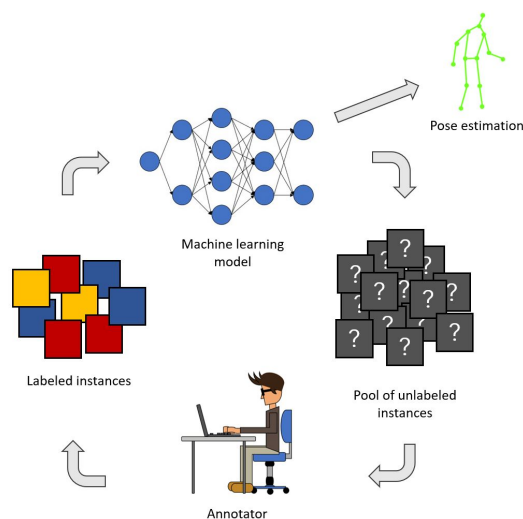


Figure 3: Active learning process. In this process, the model interactively selects some instances and asks the human annotator to label them. Then, the model is re-trained using these new labelled instances until it reaches a defined performance threshold or the budget limit.

Table 3 shows the results reported in the revised works that have used Human3.6M dataset to evaluate the model's performance. Appendix A.1 shows the outcomes obtained using single-person techniques on other datasets.

Table 3

Table summarising the results reported in the revised publications for the Human3.6M [39]

Papers	Year	MPJPE (mm) ↓
Rhodin et al. [67]	2018	131.70
Tang et al. [79]	2018	99.70
Kadkhodamohammadi and Padoy [44]	2019	57.90
Kundu et al. [48]	2020	56.10
Remelli et al. [65]	2020	30.20
Remelli et al. [65] (trained with extra data from the MPII Human Pose dataset [3])	2020	21.00
Jenni and Favaro [40]	2021	64.90
Liu et al. [53]	2021	22.50
Reddy et al. [64]	2021	18.70
Wang and Sun [83]	2022	67.20
Wang et al. [84]	2022	31.17
Bartol et al. [4]	2022	29.10
Xia and Zhang [89]	2022	17.00
Ma et al. [56]	2023	75.10
Jiang et al. [42]	2023	27.80
Zhao et al. [99]	2023	25.80
Wan et al. [82]	2023	21.10
Cai et al. [10]	2024	7.90

4.2. Multi-person approaches

This section presents the solutions developed to determine 3D poses in multi-person scenarios.

4.2.1. Geometric constraint-based methods

Belagiannis et al. [5] extended the Amin et al. [2] approach for multi-person pose estimation, using triangulation of the detected 2D body joints in the various views to create the 3D discrete state space with all body parts hypotheses for all humans in the scene. Then, the 3D Pictorial Structures (3DPS) model was used to infer the 3D human poses from the 3D body part hypotheses in the reduced state space. Later, in [7], the researchers introduced temporal consistency to their previous approach to account for estimating human body pose over time. The researchers argue that temporal consistency is highly important for estimating multiple human poses, where the trajectory of each individual is closely related to their body posture, as it aids in penalising false positive candidates. Chen et al. [15] aimed to develop

a system that can evaluate the similarity between the movements of an ordinary individual and those of someone with a motor dysfunction. To achieve this, the authors integrated temporal information into 3DPS to enhance the 3D pose estimates.

In [6], the authors based their work on their previous work [5]. Nonetheless, they used different body parametrisations by exploring the use of a 3DPS with several potential functions and also, to learn the model's parameters was used a structured Support Vector Machine (SVM) to adequately weight the different potential functions. Zhu et al. [102] also, explored the PS model, but for human motion tracking. To accomplish that, the researchers first, subtracted the background, then, used Flexible Mixtures of Parts (FMP), which is based on PS, for foreground learning to detect the human body parts and finally, to track the body parts, it was utilised Annealed Particle Filter (APF). The latest work by Belagiannis et al. [6], as mentioned, relied on a structured SVM to optimise the model parameters. In contrast, Schwarcz and Pollard [71], to simplify the hyperparameters optimisation and improve the quality of the poses estimated with triangulation, used, to determine the 3D pose, a Conditional Random Field (CRF) as a factor graph, the 3D limb locations as variables, and the limb position priors, collision terms and temporal smoothing on those joints as factors. Furthermore, for determining the 2D poses for each view, Schwarcz and Pollard took advantage of the OpenPose library [11]. On the other hand, Ershadi et al. [27] employed a bottom-up approach starting by leveraging from the DeeperCut model [38] to detect the 2D body parts. Next, a 3D search space is constructed with all detected joints and a Gaussian Mixture Model (GMM) is applied to cluster the points in order to obtain the number of people in the scene. To infer the 3D pose, a fully connected pairwise CRF with its pairwise terms defined in the 3D space and a loopy belief propagation are utilized. To alleviate the computational cost of deep neural networks developed to estimate the 3D pose, Wang et al. [84] proposed LHPE-nets. The LHPE-nets incorporate a low-span network to increase the speed of the start of the training process for the 2D pose prediction as well as a residual deep neural network trained on low-resolution data which showed to enhance network scalability and performance when compared to a ResNet-34.

To combat the inefficiency of PS-based models, Dong et al. [24] proposed a multi-way matching algorithm which leverages epipolar geometry, appearance similarity and cycle consistency to reduce the state space and eliminate false detections, resulting in a more efficient matching of 2D poses between views. Later, in [23], the researchers extend their approach to also, track the poses by introducing temporal tracking and Riemannian Extended Kalman filtering. However, their methods present some limitations, like a 2D pose can be deemed an outlier if it only appears in one view, or if there are fast movements, the tracking algorithm is unreliable. Thus, their method could not be used in applications requiring quick movement monitoring, such as sports tracking. Bridgeman et al. [9], to improve the speed of the

2D pose association across views, employed a fast greedy algorithm based only on geometric relations and then, used triangulation to generate the 3D skeletons. Although, the presented method is faster than PS-based methods, in scenarios with a small number of cameras the use of PS for joint estimation has been proven to be more precise than triangulation [23, 9]. Demonstrating the existing trade-off between speed and accuracy [23].

Xu et al. [92] focus on the application of human-robot interaction. So, for that the authors need to conjugate two tasks: estimation of the 3D human skeleton and controlling of the robot movement. Focusing on the pose estimation part, Xu et al. used a 2D pose detector to determine the pose for each view, next, used a greedy algorithm to associate the 2D poses and finally, computed the 3D pose based on paired 2D poses. To enhance efficiency and avoid pose mispairing, the authors implemented a redundancy screening phase to remove redundant pairings, as well as iteration reversal which is used to double-check the validity of the current state; if the state fails this check, the iteration returns to its backup state.

To tackle the issue of swiftly and accurately predicting the 3D pose in crowded scenarios, Chen et al. [14] used the Jonker-Volgenant algorithm to first, associate the foot joints across the various views, and then, used that information and the human body kinematics to find the matches for the rest of the joints. Lastly, to regress the 3D pose, the researchers refined the triangulation method by introducing Maximum A Posteriori (MAP) optimisation that takes into account the uncertainties of the 2D estimations and imposes the average lengths of the 3D bones.

Huang et al. [35] proposed a method which allows a back-propagation of the gradients from the 3D estimation step to the 2D pose detection, enabling end-to-end training of the model. Also, another contribution is the proposed bottom-up dynamic matching algorithm that constructs 3D pose sub-spaces by projecting each pair of 2D poses using triangulation into 3D poses. The matching 3D poses are then identified using a distance-based clustering approach.

As for Chu et al. [18], the researchers introduced a method to lessen the computational burden imposed by the matching process. The approach consisted of the use of temporal consistency and part-aware measurement to be able to exploit previously obtained 3D poses to discover better 2D-3D correspondence across perspectives. Additionally, to remove possible outliers or noisy data, a joint filter is applied, improving the robustness of the 3D reconstruction. On the other hand, Dehaeck et al. [20] showed that it's possible to obtain a reliable cross-view matching algorithm by relying only on geometric constraints, like the Sampson error which allows to compute the distance between predicted points from two distinct views. Furthermore, the authors claim that solving the matching problem between views requires at least three perspectives, however, if only two of them are free from occlusions, the trustworthiness of the matches drops. Xu and Kitani [93] suggested employing multi-view

geometry to reduce the solution space for cross-view matching. Thus, the authors established several requirements: each individual must be within the field of view of at least two cameras, no person can have more matches than the number of available cameras, and individuals from the same view cannot be matched. Then, to enhance the association of the 2D poses across the several views, a self-validation method is used, exploiting the correspondences with higher quality from all camera pairs. Lastly, the 3D poses from different pairs of cameras are triangulated to generate the final 3D pose, which is then refined via bundle adjustment. This methodology culminates in a method robust to distinct camera settings without requiring to know any calibration parameters. Ershadi-Nasab et al. [26] adopted an adversarial learning methodology aiming to estimate the 3D pose without requiring any camera calibration. The model is composed of a generator which estimates the 3D pose and attempts to create estimates that the discriminator cannot differentiate from the ground-truth poses. Thus, the generator calculates the 2D Euclidean distance and 2D angular difference matrices before mapping each of them to the equivalent 3D version which are subsequently utilized to generate the 3D pose. Also, for the generator to become more robust to occlusions and improve the 3D pose estimation, a Procrustes analysis was used to allow the association of the poses over several viewpoints. The discriminator compares the 3D Euclidean distance and 3D angular difference matrices of the generated pose with the ground-truth and determines if they are identical.

Other works have explored techniques to select the best views regarding occlusions to more accurately estimate the 3D pose [79, 28, 83]. Fan et al. [28] developed MAO-Pose, a self-supervised method capable of managing camera positions. Therefore, the various cameras are encouraged to choose the best perspective for the visibility of the joints and to diversify their choices of viewpoints in comparison to the perspectives chosen by the other cameras, in order to promote a broad range of views. Furthermore, a communication system called Consensus is introduced to allow the cameras to exchange their position information and assist the next camera in optimising its position plan by knowing how the other cameras are going to be placed. Wang et al. [83], on the other hand, introduced Smart-VPoseNet, a model that relies just on one view to reconstruct the 3D pose. However, the used perspective is chosen dynamically from all available viewpoints in a multi-view system. The choosing criteria that Smart-VPoseNet follows are the number of visible joints, the degree of stretch of the human body and the level of affinity between the perspective and the model. These three criteria can be used individually or in conjunction depending on the characteristics of the dataset. Furthermore, the authors claim that their methodology provides a basis for a possible two-view fusion system.

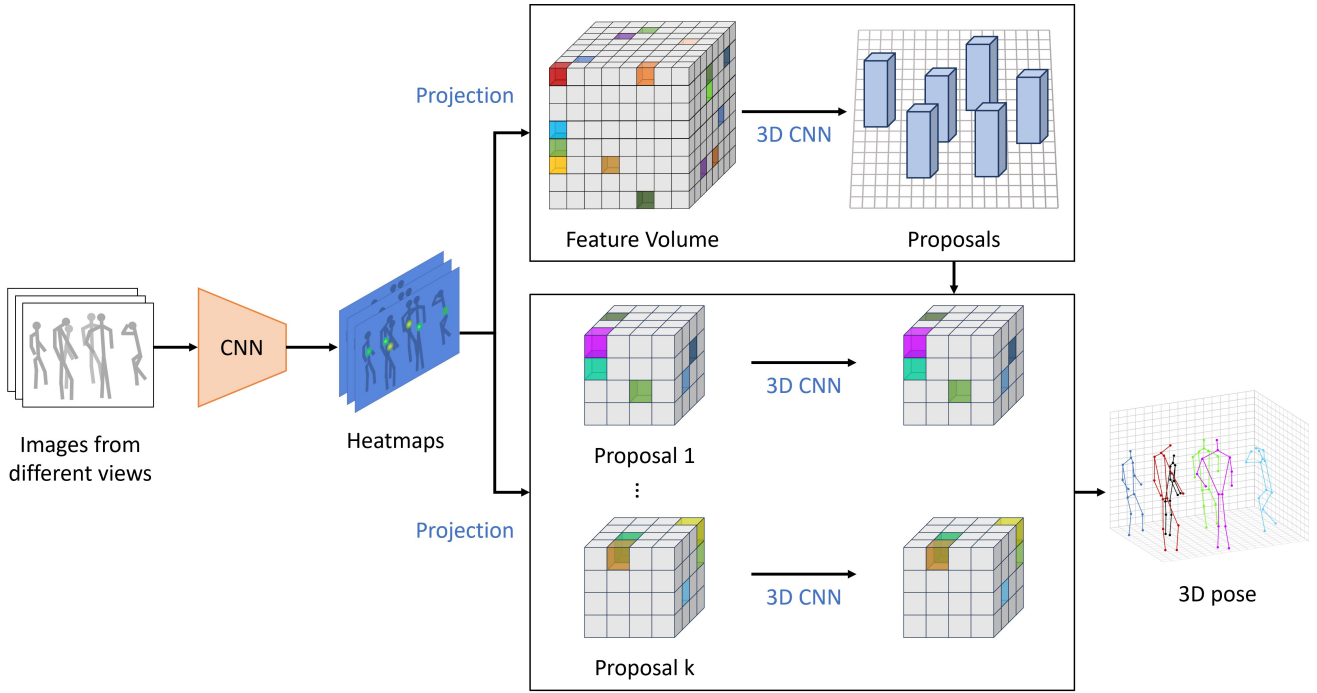


Figure 4: Overview of the VoxelPose architecture (image adapted from [81])

4.2.2. Voxel-based approaches

In [81], Tu et al. introduced VoxelPose (see Figure 4), a method that completely avoids erroneous 2D pose associations of different views, by directly working on the 3D space. Thus, the model receives as input the images from the various perspectives and generates the corresponding 2D heatmaps. Next, these heatmaps are projected into the 3D space to form a 3D feature volume which serves as input for the Cuboid Proposal Network (CPN) that will output a 3D cuboid proposal for each person in the scene. Finally, finer-grained cuboids are created, to enable a more accurate estimation of the pose, and fed to the Pose Regression Network (PRN) to obtain the 3D poses.

The robustness of the method against occlusions and the superior performance compared to previous approaches has attracted the community to explore this methodology. Thus, various subsequent works are based on this architecture, such as [21, 94, 104, 98, 64, 16, 103].

Deng et al. [21] in order to make the VoxelPose model robust to domain shift have proposed to include a domain adaptation component, a dropout mechanism and a transferable parameter learning. These new additions will enable the learning of representative features across different domains, while, also, mitigating the adverse consequences of learning domain-specific information. Nonetheless, although it improves cross-domain efficiency and reduces the need for manually labelled data, the training overhead is quite high, restricting its applicability to settings requiring highly demanding processing processes, and this becomes even more pronounced as the number of perspectives increases.

On the other hand, Faster VoxelPose [94] focused on improving the VoxelPose's speed by avoiding the use of 3D CNN. In order to do so, the feature volume belonging to each individual had to be identified, and then, re-projected to 2D space independently. However, the method is not robust to the decrease in the number of views, leading to a significant performance drop. Thus, to address that Zhuang and Zhou [104] proposed FasterVoxelPose+, introducing two changes to the Faster VoxelPose model: a Depth-wise Projection Decay (DPD) and an Encoder-Decoder Network (EDN). DPD is a projection technique that adds extra depth information to the projection of the 2D pose heatmaps into the 3D voxel features. While EDN consists of a 2D CNN able to combine multi-scale information, allowing 2D re-projected voxel features to be processed in different phases and consequently, reaching more accurate 3D bounding boxes estimates and 2D poses. In the case of VoxelTrack [98], the authors expanded on the VoxelPose approach to include tracking 3D postures throughout time. Furthermore, a more robust 2D backbone network and extra 3D heatmap supervision of all joints are added to try to improve the 3D pose estimations and, to enhance inference speed, sparse 3D CNNs are exploited. However, when the number of cameras decreases, all of these approaches still suffer a decline in performance, with this effect being less pronounced in FasterVoxelPose+. TeseTrack [64] is, also, less influenced by this, since it integrates temporal information via the 4D spatio-temporal CNN. This makes the model more resilient to occlusions, better at predicting joint locations, and able to cope with appearance ambiguities in just one frame.

Regarding the work of Zhu et al. [103], the VoxelPose approach was also, followed to compute for each human proposal, the respective feature volume. Nonetheless, as their objective was to create a reliable method to work in crowded environments, the authors have proposed a three-stage strategy to refine the 3D poses. Thus, the initial step was to generate finer-grained and narrower feature volumes in the region around each human proposal. In the second-stage, the Voxel Hourglass Network used those feature volumes to generate 3D heatmaps and tag-maps. Then, a 3D Associative Embedding was employed to combine the information provided by the heatmaps and tag-maps to produce a coarse 3D pose. In the third-stage, a refinement layer is utilised to refine the 3D pose given by the previous step. The authors demonstrated that the incorporation of 3D tag-maps resulted in the elimination of undesired joints coming from other people in the scene which, consequently, lowered the amount of mismatched joints.

Additionally, inspired by VoxelPose, Wang et al. [86] introduced MvP, a transformer-based model for solving the multi-person 3D pose estimation task. This method directly predicted the 3D skeleton by encoding the joints as learnable query embeddings and joining them with the features extracted from the input images. Furthermore, to increase the model's performance, the suggested transformer used a projective attention mechanism based on geometrical information in conjunction with a RayConv operation to precisely fuse the cross-view data for each joint. The authors point out some drawbacks of their approach which are the lack of robustness to generalize for new camera perspectives and a high demand for training data. Another transformer-based approach, based on VoxelPose is Volumetric Transformer Pose Estimator (VTP) [16]. The creation of this model aimed to solve the high computational cost associated with applying self-attention directly to volumetric representations. To overcome this, Sparse Sinkhorn Attention (SSA) mechanism was exploited as it provides quasi-global local attention. To do this, the input sequence is divided into blocks, then the correlation between them is learnt, and finally, SSA uses this information to understand how to reorganise and classify the blocks. The authors have concluded that by applying SSA the memory consumption was reduced, allowing to efficiently apply self-attention to the volumetric representations.

4.2.3. Plane sweep stereo-based models

To create a faster and less computationally expensive algorithm compared to VoxelPose, Lin and Lee [50] proposed a framework based on plane sweep stereo to add person-level and joint-level depth information to the 2D poses generated for each viewpoint, see Figure 5. Then, the 2D poses and respective depth information are back-projected to create the 3D pose, reducing the computational burden of pose association. Extending this approach to work with unlabelled datasets, de França Silva et al. [30] changed the loss function used on the previously presented plane sweep stereo method to be able to learn the 3D poses in an unsupervised way. Thus, instead of computing the difference

between the generated 3D pose and the ground-truth, this novel loss function employs re-projection error between the 2D projection of the 3D pose with the 2D pose estimated for that perspective. The authors besides demonstrating the potential of this approach to learn from data without annotations, also, showed the potential of Adabelief to provide quicker convergences and better performances than the Adam optimiser. Later de França Silva et al. [31] extended their work by exploring a matching method that uses ground points related to each individual to match the target with the reference view. Additionally, the authors incorporated the smooth L_1 loss for computing the re-projection error of the 2D poses. These modifications yielded a significant performance enhancement compared to the previous version, while also showcasing the potential of this method to cope with unlabeled data. However, it is noteworthy that this approach necessitates the knowledge of camera parameters in order to calculate the loss.

Zhou et al. [101] also, took advantage of the plane sweep stereo method to get the depth score matrices, and subsequently obtain the 3D pose by back-projecting the 2D poses with the corresponding depth information. However, to optimise the prediction of all joints, particularly those most affected by occlusions or other external factors that may impair their detection, the authors employed an attention channel mechanism and an optimal calibration method based on the dependency relationship between the joints and the individual. This strategy promoted channel-wise feature recalibration by adjusting the weights given to each channel, allowing the model to understand the long dependency relationship between joints and improve the detection of the most difficult joints.

Table 4 reports the results for all revised works that have used Campus or Shelf dataset to assess the performance of their model. Appendix A.2 presents the outcomes obtained with multi-person approaches on other datasets.

5. Multi-modal approaches

This section presents methods that have used other sensors rather than RGB cameras to estimate the 3D pose.

5.1. Different type of cameras

Some researchers have tackled the 3D pose estimation task using types of camera sensors, such as RGB-D cameras [12, 37], ToF cameras [33], or 360° cameras [73] which provide images that differ from the typical RGB images. These types of cameras can capture more information which can be advantageous for the estimation of the pose. For example, Shere et al. [73] created a method to determine the 3D pose using two 360° cameras. The authors state that this type of camera is especially advantageous since it can capture the whole scene without requiring a huge number of cameras while simultaneously providing accurate depth information. Thus, they used temporal information to associate the 2D poses and mitigate inaccuracies. Although their method has been developed to be used with data outputted by 360° cameras, data from other types of cameras may also be

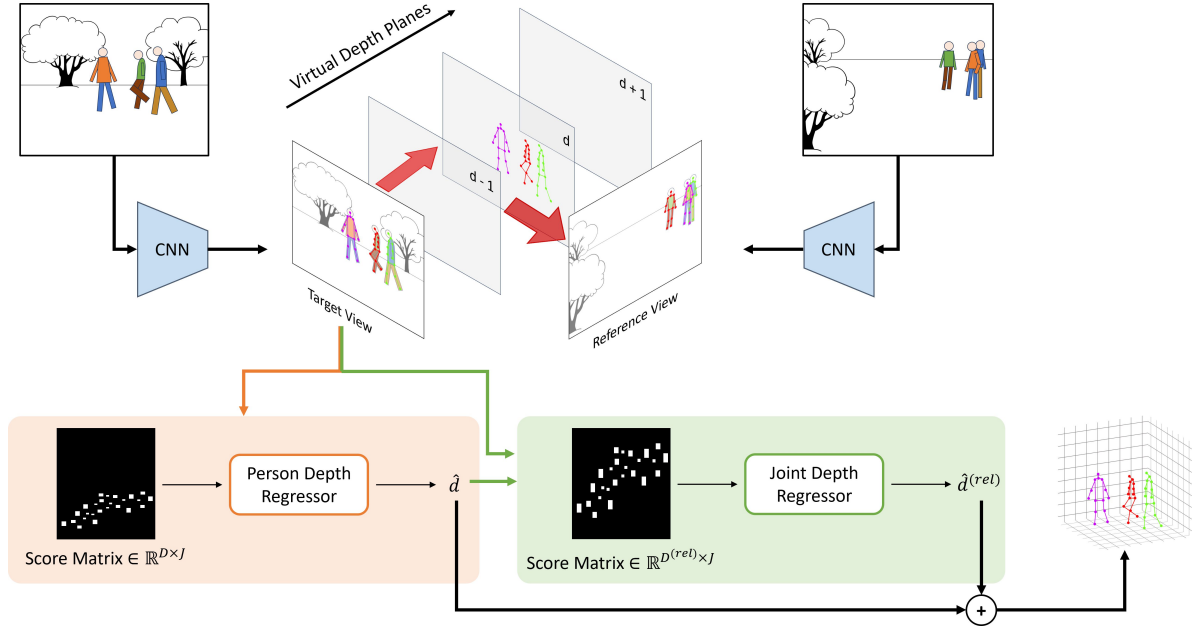


Figure 5: Overview of the plane sweep stereo-based method followed by Lin and Lee (image adapted from [50])

used, however, it will require the data to go through a costly re-projection step. In the case of Carraro et al. [12], they have estimated the 3D human pose using an array of RGB-D cameras. This allowed them to leverage depth information to compute the 3D pose from the 2D poses generated by using a single-view pose estimation algorithm and the cameras' extrinsic calibration parameters. Additionally, the authors used Kalman Filters to track the poses over time. The developed system thus allows the estimation of multiple people in real-time. Hwang et al. [37] have also, taken advantage of the depth information given by the RGB-D cameras to optimise the process of the cross-view matching of the 2D poses. Then, to be able to deploy this method in real-world, the authors have employed a system similar to [36].

Regarding the work of Hassan et al. [33], the authors have used ToF cameras which provide infra-red intensity images along with depth information. The use of infra-red intensity images allows the system to be more robust to occlusions, material reflectivity, and lighting conditions in comparison to systems that utilise RGB images. Besides, the authors have proven that the use of intensity images as input is more reliable for estimating the 2D poses and subsequently, projecting them to construct the 3D pose than the depth images. However, in case a joint cannot be determined, the model takes advantage of the depth information to get the position of the missing joint.

5.2. Wireless sensors

On the other hand, some researchers have opted to use other types of sensors which can overcome some limitations vision-based methods suffer. Thus, the use of wireless communications to complete this task has been explored, because they aren't affected by occlusions, privacy concerns

or bad illumination conditions which are some challenges vision-based methods have to face [77, 91, 90].

Typically, systems designed to rebuild 3D poses using wireless signals, such as RF [77, 91, 90] or Wi-Fi [87, 66], include a camera that is synchronised with the wireless signals. Nonetheless, the researchers only used the camera data to produce ground-truth 3D poses with which to compare the skeletons generated using wireless signals [87, 66, 77, 91, 90]. The typical pipeline for approaches that use these types of signals starts with transforming the input signal into images by, for example, extracting the channel-state information or the angle of arrival spectrums. Then, a method from the computer vision domain is employed to obtain the final 3D pose [87, 66, 77, 91, 90].

6. Conclusion

In summary, most existing methods use a three-step methodology where first, the 2D pose is regressed from the input images, then, the 2D poses predicted for the different views are associated and finally, the 3D pose is constructed. However, this type of strategy can lead to unreliable 3D poses due to mismatches and erroneous 2D poses. Therefore, some methods have surpassed this problem by completely avoiding this step and working directly on the 3D space [81]. Nevertheless, operations in the volumetric space become more computationally expensive, which might restrict their application in real-world settings. On the other hand, another methodology that has been utilised to combat this problem is the selection of views. So, the model only uses, to predict the pose, the views that provide better visualisation of the human subjects. Consequently, by using just some of the available views, the computational burden is also reduced.

Table 4

Table summarising the results reported in the revised publications for the Campus [5] and Shelf [5] datasets

Papers	Year	Campus — PCP (%) \uparrow				Shelf — PCP (%) \uparrow			
		Actor 1	Actor 2	Actor 3	Average	Actor 1	Actor 2	Actor 3	Average
Belagiannis et al. [5]	2014	82.00	72.00	73.00	75.60	66.00	65.00	83.00	71.30
Belagiannis et al. [7]	2015	83.00	73.00	78.00	78.00	75.00	67.00	86.00	76.00
Belagiannis et al. [6]	2016	93.45	75.65	84.37	84.49	75.26	69.68	87.59	77.51
Szwarcz and Pollard [71]	2018	86.55	82.54	88.14	85.15	88.34	85.26	91.30	88.92
Ershadi-Nasab et al. [27]	2018	94.18	92.89	84.62	90.56	93.29	75.85	94.83	87.99
Bridgeman et al. [9]	2019	91.84	92.71	93.16	92.57	99.68	92.79	97.72	96.73
Dong et al. [24]	2019	97.60	93.30	98.00	96.30	98.80	94.10	97.80	96.90
Tu et al. [81]	2020	97.60	93.80	98.80	96.70	99.30	94.10	97.60	97.00
Huang et al. [35]	2020	97.96	94.81	97.39	96.71	98.75	96.22	97.20	97.39
Wang et al. [86]	2021	98.20	94.10	97.40	96.60	99.30	95.10	97.80	97.40
Zhang et al. [98]	2021	98.10	93.70	98.30	96.70	98.60	94.90	97.70	97.10
Chu et al. [18]	2021	98.37	93.76	98.26	96.79	99.14	95.41	97.64	97.39
Lin and Lee [50]	2021	98.40	93.70	99.00	97.00	99.30	96.50	98.00	97.90
Reddy et al. [64]	2021	97.90	95.20	99.10	97.40	99.10	96.30	98.30	98.20
Ershadi Nasab et al. [26]	2021	98.41	95.12	98.82	97.45	99.83	94.91	98.33	97.69
de França Silva et al. [30]	2022	96.90	87.80	88.90	91.20	—	—	—	—
Ye et al. [94]	2022	96.50	94.10	97.90	96.20	99.40	96.00	97.50	97.60
Dong et al. [23]	2022	97.60	93.30	98.00	96.30	98.80	94.10	97.80	96.90
Zhou et al. [101]	2022	98.60	94.00	99.20	97.30	99.40	97.30	98.20	98.30
Xu and Kitani [93]	2022	99.00	94.70	99.60	97.80	99.60	95.20	98.50	97.80
Chen et al. [16]	2023	97.60	93.10	98.10	96.30	99.30	95.10	97.40	97.30
Zhuang and Zhou [104]	2023	97.40	93.60	98.10	96.40	99.00	96.30	97.70	97.70
Deng et al. [21]	2023	85.10	86.30	78.40	83.20	96.50	94.10	97.70	96.10
de França Silva et al. [31]	2023	98.40	93.40	98.60	96.80	—	—	—	—
Chen et al. [15]	2024	—	—	—	—	98.60	95.80	97.90	97.40

Another limitation that most proposed methods still have to face is the dependence on the camera setup and camera's calibration parameters, making most existing models unable to generalise to new viewpoints. To surpass this, researchers have exploited geometric multi-view consistency, stochasticity-based triangulation, adversarial learning and self-supervised learning methods.

Regarding the scarcity of 3D labelled datasets, methods that learn using a low level of supervision have been suggested to address this challenge. Nonetheless, some of those methods still depend on some 2D labelled data. On the other hand, the use of active learning has also, been suggested to overcome this issue. This strategy allows to dynamically acquire labels for unlabelled instances to boost model accuracy while requiring the least amount of annotation labour feasible. Nevertheless, only one work was found

to employ this strategy, thus, more research is still required to determine the full potential of this technique for this task.

Even though many works have focused on solving this problem, the occurrence of occlusion still limits the model's performance in many cases. Temporal consistency has been widely used to track poses over time and also, to overcome the occlusion problem. Nonetheless, as pointed out by [61], the use of this approach might suppress sudden and minor movements which can negatively impact the model's performance and also make it unsuitable for applications where the detection of those movements might be crucial, such as surveillance systems. Besides temporal consistency, the long-range dependencies between joints and the person, and the use of depth information have been proposed to improve the model's robustness against occlusions.

Finally, the use of more sophisticated types of cameras that can give additional information beyond RGB images

has been shown to be able to provide reliable 3D pose estimations. These types of cameras have not yet been very explored, nonetheless, their employment could be advantageous because, according to the found works, the RGB-D, ToF and 360° cameras, can directly provide depth information. By providing depth information directly as input, the computational cost associated with models using depth information can be substantially reduced, as the need for depth calculation will no longer be required. Regarding other types of signals, some researchers have explored the use of wireless signals to estimate the 3D pose. However, the association of information retrieved by wireless sensors with visual information given by cameras has not yet been investigated, leaving space for an innovative multi-modal approach combining both domains.

Thus, it's possible to conclude that, although various techniques have been proposed to try to overcome most challenges inherent to the estimation of the 3D pose, none of the existing approaches can balance high accuracy, quick inference, and low computational cost. So, the best model depends on the desired application, due to the trade-off between performance and complexity. Therefore, more research work is still needed in this area to find a suitable methodology for different application scenarios. The combination of a multi-modal approach with active learning may be the future for an efficient and accurate solution.

Acknowledgments

This work has received funding from the European Union's Horizon Europe research and innovation programme under the Grant Agreement 101094831 - CONVERGE project and by National Funds through the Portuguese funding agency, FCT-Foundation for Science and Technology Portugal, a PhD Grant Number 2023.02851.BD.

A. Datasets - Benchmarking

This section includes a summary of the results reported in the reviewed publications.

A.1. Single-person 3D pose estimation

Table 5, Table 6, Table 7 and Table 8 present the results for the dataset MPI-INF-3DHP, KTH Multiview Football II, HumanEva and Total Capture, respectively.

Table 5

Performance of the revised methods in the MPI-INF-3DHP dataset

Papers	Year	PCK (%) ↑	AUC (%) ↑	MPJPE (mm) ↓
Kundu et al. [48]	2020	81.90	52.60	89.80
Wang et al. [84]	2022	—	—	112.36
Wang and Sun [83]	2022	—	—	94.70
Ma et al. [56]	2023	74.60	40.40	—
Cai et al. [10]	2024	—	—	5.40

Table 6

Performance of the revised methods in the KTH Multiview Football II dataset

Papers	Year	# Cameras	PCP (%) ↑				
			Upper arms	Lower arms	Upper Legs	Lower Legs	All parts (average)
Belagiannis et al. [5]	2014	2	64.00	50.00	75.00	66.00	63.80
		3	68.00	56.00	78.00	70.00	68.00
Belagiannis et al. [6]	2016	2	96.00	68.00	98.00	88.00	87.50
		3	98.00	72.00	99.00	92.00	90.30
Ershadi-Nasab et al. [27]	2018	3	97.47	94.89	100.00	99.00	98.14
Ershadi Nasab et al. [26]	2021	3	100.00	99.60	100.00	99.60	99.80

Table 7

3D error (mm) ↓ of the revised methods in the HumanEva dataset

Papers	Year	Sequence 1				Sequence 2			Sequence 3		
		Walk	Jog	Balance	Box	Walk	Jog	Balance	Walk	Jog	Combo
Sigal et al. [74]	2010	76.0	85.0	86.0	—	60.0	93.0	80.0	—	—	—
Amin et al. [2]	2013	54.5	—	—	47.7	50.2	—	—	54.7	54.0	51.8
Belagiannis et al. [5]	2014	68.3	—	—	62.7	—	—	—	—	—	—
Belagiannis et al. [6]	2016	68.3	—	—	62.7	—	—	—	—	—	—
Mehrizi et al. [58]	2018	40.4	43.0	—	—	23.5	45.1	—	33.4	30.9	—

Table 8
MPJPE (mm) ↓ of the revised methods in the Total Capture dataset

Papers	Year	Seen Cameras (1, 3, 5, 7)						Unseen Cameras (2, 4, 6, 8)							
		Seen Subject 1, 2, 3			Unseen Subject 4, 5			Avg.	Seen Subject 1, 2, 3			Unseen Subject 4, 5			Avg.
		W2	FS3	A3	W2	FS3	A3		W2	FS3	A3	W2	FS3	A3	
Remelli et al. [65]	2020	10.60	30.40	16.30	27.00	65.00	34.20	27.50	22.40	47.10	27.80	39.10	75.70	43.10	38.20
Wan et al. [82]	2023	13.00	24.00	17.00	23.00	41.00	29.00	23.00	—	—	—	—	—	—	—
Cai et al. [10]	2024	5.50	15.00	5.68	18.10	37.60	20.60	15.00	22.10	35.40	23.40	23.20	42.60	28.40	28.30

Avg. - Average
Testing sequences: W2 - Walking2, FS3 - Freestyle3, A3 - Acting3.
Training sequences: ROM1,2,3; Walking1,3; Freestyle1,2; Acting1,2 and Running1 using subjects 1, 2 and 3.

A.2. Multi-person 3D pose estimation

Table 9 and Table 10 present the results for the dataset UMPM and CMU Panoptic, respectively.

Table 9
Performance of the revised methods in the UMPM dataset

Papers	Year	Actors	PCP (%) ↑						
			Head	Torso	Upper arms	Lower arms	Upper Legs	Lower Legs	Average
Ershadi-Nasab et al. [27]	2018		95.87	98.53	92.42	84.92	94.23	86.36	91.02
Ershadi Nasab et al. [26]	2021		99.40	99.70	95.30	89.80	96.60	90.40	94.30

Papers	Year	Actors	UMPM sequence: p3-chair-11 — PCP (%) ↑						
			Head	Torso	Upper arms	Lower arms	Upper Legs	Lower Legs	Average
Ershadi-Nasab et al. [27]	2018	A1	94.76	96.82	91.24	83.78	92.45	85.56	89.76
		A2	95.87	97.28	95.12	83.89	93.76	85.12	89.89
Ershadi Nasab et al. [26]	2021	A1	99.42	99.34	98.89	91.56	97.11	96.32	96.65
		A2	98.31	99.20	99.10	90.22	96.45	94.65	95.83

Table 10
Performance of the revised methods in the CMU Panoptic dataset

#Views	Paper	Year	MPJPE (mm) ↓	AP ₂₅ ↑	AP ₅₀ ↑	AP ₇₅ ↑	AP ₁₀₀ ↑	AP ₁₂₅ ↑	AP ₁₅₀ ↑	mAP ↑
2	Wang et al. [86]	2021	34.80	37.70	—	—	93.00	—	—	—
	Zhu et al. [103]	2023	47.42	25.51	62.03	77.89	86.14	90.16	92.39	72.35
	Zhuang and Zhou [104]	2023	42.53	31.25	65.63	—	93.51	—	96.12	—
3	Tu et al. [81]	2020	24.29	58.94	93.88	—	98.45	—	99.32	—
	Wang et al. [86]	2021	21.10	71.80	—	—	95.10	—	—	—
	Zhang et al. [98]	2021	24.93	49.09	92.44	—	97.62	—	—	—
	Ye et al. [94]	2022	26.13	53.68	91.89	—	97.40	—	98.30	—
	Zhu et al. [103]	2023	33.03	34.98	76.72	89.37	93.87	96.06	97.24	81.37
	Zhuang and Zhou [104]	2023	24.98	57.23	92.21	—	97.83	—	98.32	—
4	Fan et al. [28]	2021	113.60	—	—	—	—	—	—	—
	Wang et al. [86]	2021	19.30	84.10	—	—	96.70	—	—	—
	Zhang et al. [98]	2021	20.35	66.20	96.34	—	99.47	—	—	—
	Ye et al. [94]	2022	21.12	73.95	97.02	—	99.21	—	99.35	—
	Zhu et al. [103]	2023	23.89	52.84	90.80	96.63	97.85	98.46	98.88	89.24
	Zhuang and Zhou [104]	2023	20.95	75.92	97.86	—	99.32	—	99.40	—
5	Tu et al. [81]	2020	17.68	83.59	98.33	—	99.76	—	99.91	—
	Fan et al. [28]	2021	94.21	—	—	—	—	—	—	—
	Lin and Lee [50]	2021	16.75	92.12	98.96	—	99.81	—	99.84	—
	Reddy et al. [64]	2021	7.30	—	—	—	—	—	—	—
	Wang et al. [86]	2021	15.80	92.30	96.60	—	97.50	—	97.70	—
	Zhang et al. [98]	2021	16.97	85.88	98.31	—	99.54	—	—	—
	Ye et al. [94]	2022	18.26	85.22	98.08	—	99.32	—	99.48	—
	Chen et al. [16]	2023	17.62	83.79	97.14	—	98.15	—	98.40	—
	Zhu et al. [103]	2023	18.88	61.28	95.10	98.70	99.39	99.76	99.87	92.35
Zhuang and Zhou [104]	2023	17.42	86.25	98.45	—	99.77	—	99.82	—	
6	Fan et al. [28]	2021	87.53	—	—	—	—	—	—	—
7	Fan et al. [28]	2021	84.02	—	—	—	—	—	—	—
8	Fan et al. [28]	2021	80.81	—	—	—	—	—	—	—

Sequences used by Tu et al. [81], Reddy et al. [64], Ye et al. [94], Zhang et al. [98], Chen et al. [16], Lin and Lee [50], Zhuang and Zhou [104]

Train set: "160422_ultimatum1", "160224_hagglng1", "160226_hagglng1", "161202_hagglng1", "160906_ian1", "160906_ian2", "160906_ian3", "160906_band1", "160906_band2" and "160906_band3".

Test set: "160906_pizza1", "160422_hagglng1", "160906_ian5" and "160906_band4".

Wang et al. [86] – training set includes the same sequences presented above except for "160906_band3". The test sequences are the same.

Fan et al. [28] – training set: "Mafia", validation set: "Mafia" and "Ultimatum" and testing set: "Mafia", "Ultimatum" and "Hagglng".

Zhu et al. [103] – training set: "160422_ultimatum1" and testing set: "160906_pizza1".

References

- [1] van der Aa, N., Luo, X., Giezeman, G., Tan, R., Veltkamp, R., 2011. Umpm benchmark: A multi-person dataset with synchronized video and motion capture data for evaluation of articulated human motion and interaction, in: 2011 IEEE International Conference on Computer Vision Workshops (ICCV Workshops), pp. 1264–1269. doi:10.1109/ICCVW.2011.6130396.
- [2] Amin, S., Andriluka, M., Rohrbach, M., Schiele, B., 2013. Multi-view pictorial structures for 3d human pose estimation, in: British Machine Vision Conference. URL: <https://api.semanticscholar.org/CorpusID:8474682>, doi:10.5244/C.27.45.
- [3] Andriluka, M., Pishchulin, L., Gehler, P., Schiele, B., 2014. 2d human pose estimation: New benchmark and state of the art analysis, in: IEEE Conference on Computer Vision and Pattern Recognition (CVPR).
- [4] Bartol, K., Bojanić, D., Petković, T., Pribanić, T., 2022. Generalizable human pose triangulation, in: Proceedings of IEEE/CVF Conf. on Computer Vision and Pattern Recognition (CVPR).
- [5] Belagiannis, V., Amin, S., Andriluka, M., Schiele, B., Navab, N., Ilic, S., 2014. 3d pictorial structures for multiple human pose estimation, in: 2014 IEEE Conference on Computer Vision and Pattern Recognition, pp. 1669–1676. doi:10.1109/CVPR.2014.216.
- [6] Belagiannis, V., Amin, S., Andriluka, M., Schiele, B., Navab, N., Ilic, S., 2016. 3d pictorial structures revisited: Multiple human pose estimation. IEEE Transactions on Pattern Analysis and Machine Intelligence 38, 1929–1942. doi:10.1109/TPAMI.2015.2509986.
- [7] Belagiannis, V., Wang, X., Schiele, B., Fua, P., Ilic, S., Navab, N., 2015. Multiple human pose estimation with temporally consistent 3d pictorial structures, in: Computer Vision - ECCV 2014 Workshops, Springer International Publishing, Cham, pp. 742–754.
- [8] Ben Gamra, M., Akhloufi, M.A., 2021. A review of deep learning techniques for 2d and 3d human pose estimation. Image and Vision Computing 114, 104282. URL: <https://www.sciencedirect.com/science/article/pii/S0262885621001876>, doi:10.1016/j.imavis.2021.104282.
- [9] Bridgeman, L., Volino, M., Guillemaut, J.Y., Hilton, A., 2019. Multi-person 3d pose estimation and tracking in sports, in: 2019 IEEE/CVF Conference on Computer Vision and Pattern Recognition Workshops (CVPRW), pp. 2487–2496. doi:10.1109/CVPRW.2019.00304.
- [10] Cai, Y., Zhang, W., Wu, Y., Jin, C., 2024. Fusionformer: A concise unified feature fusion transformer for 3d pose estimation. Proceedings of the AAAI Conference on Artificial Intelligence 38, 900–908. URL: <https://ojs.aaai.org/index.php/AAAI/article/view/27849>, doi:10.1609/aaai.v38i2.27849.
- [11] Cao, Z., Simon, T., Wei, S.E., Sheikh, Y., 2017. Realtime multi-person 2d pose estimation using part affinity fields, in: CVPR.
- [12] Carraro, M., Munaro, M., Burke, J., Menegatti, E., 2019. Real-time marker-less multi-person 3d pose estimation in rgb-depth camera networks, in: Intelligent Autonomous Systems 15, Springer International Publishing, Cham, pp. 534–545.
- [13] Chavdarova, T., Baqué, P., Bouquet, S., Maksai, A., Jose, C., Bagautdinov, T., Lettry, L., Fua, P., Van Gool, L., Fleuret, F., 2018. Wild-track: A multi-camera hd dataset for dense unscripted pedestrian detection, in: 2018 IEEE/CVF Conference on Computer Vision and Pattern Recognition, pp. 5030–5039. doi:10.1109/CVPR.2018.00528.
- [14] Chen, H., Guo, P., Li, P., Lee, G.H., Chirikjian, G., 2020a. Multi-person 3d pose estimation in crowded scenes based on multi-view geometry, in: Computer Vision – ECCV 2020, Springer International Publishing, Cham, pp. 541–557.
- [15] Chen, L., Liu, T., Gong, Z., Wang, D., 2024. Movement function assessment based on human pose estimation from multi-view. Computer Systems Science and Engineering 48, 321 – 339. URL: <https://www.scopus.com/inward/record.uri?eid=2-s2.0-85191093708&doi=10.32604/2fcsse.2023.037865&partnerID=40&md5=9f2e54e75483da59b7207dcb224d63f5>, doi:10.32604/csse.2023.037865.
- [16] Chen, Y., Gu, R., Huang, O., Jia, G., 2023. Vtp: Volumetric transformer for multi-view multi-person 3d pose estimation. Applied Intelligence 53, 26568–26579. doi:10.1007/s10489-023-04805-z.
- [17] Chen, Y., Tian, Y., He, M., 2020b. Monocular human pose estimation: A survey of deep learning-based methods. Computer Vision and Image Understanding 192, 102897. URL: <https://www.sciencedirect.com/science/article/pii/S1077314219301778>, doi:10.1016/j.cviu.2019.102897.
- [18] Chu, H., Lee, J.H., Lee, Y.C., Hsu, C.H., Li, J.D., Chen, C.S., 2021. Part-aware measurement for robust multi-view multi-human 3d pose estimation and tracking, in: Proceedings of the IEEE/CVF Conference on Computer Vision and Pattern Recognition (CVPR) Workshops, pp. 1472–1481.
- [19] Chunhui, L., Yueyu, H., Yanghao, L., Sijie, S., Jiaying, L., 2017. Pku-mmd: A large scale benchmark for continuous multi-modal human action understanding. arXiv preprint arXiv:1703.07475.
- [20] Dehaeck, S., Domken, C., Bey-Temsamani, A., Abedrabbo, G., 2022. A strong geometric baseline for cross-view matching of multi-person 3d pose estimation from multi-view images, in: Image Analysis and Processing – ICIAP 2022, Springer International Publishing, Cham, pp. 77–88.
- [21] Deng, J., Yao, H., Shi, P., 2023. Enhanced 3d pose estimation in multi-person, multi-view scenarios through unsupervised domain adaptation with dropout discriminator. Sensors (Basel, Switzerland) 23. URL: <https://www.scopus.com/inward/record.uri?eid=2-s2.0-85175273967&doi=10.3390%2Fs23208406&partnerID=40&md5=71c6d12d63fcbdc0b81aaf0a0fb8576c>, doi:10.3390/s23208406.
- [22] Desmarais, Y., Mottet, D., Slangen, P., Montesinos, P., 2021. A review of 3d human pose estimation algorithms for markerless motion capture. Computer Vision and Image Understanding 212, 103275. URL: <https://www.sciencedirect.com/science/article/pii/S1077314221001193>, doi:10.1016/j.cviu.2021.103275.
- [23] Dong, J., Fang, Q., Jiang, W., Yang, Y., Huang, Q., Bao, H., Zhou, X., 2022. Fast and robust multi-person 3d pose estimation and tracking from multiple views. IEEE Transactions on Pattern Analysis and Machine Intelligence 44, 6981–6992. doi:10.1109/TPAMI.2021.3098052.
- [24] Dong, J., Jiang, W., Huang, Q., Bao, H., Zhou, X., 2019. Fast and robust multi-person 3d pose estimation from multiple views. arXiv:1901.04111.
- [25] Duarte, A., Palaskar, S., Ventura, L., Ghadiyaram, D., DeHaan, K., Metz, F., Torres, J., Giro-i Nieto, X., 2021. How2Sign: A Large-scale Multimodal Dataset for Continuous American Sign Language, in: Conference on Computer Vision and Pattern Recognition (CVPR).
- [26] Ershadi Nasab, S., Kasaei, S., Sanaei, E., 2021. Uncalibrated multi-view multiple humans association and 3d pose estimation by adversarial learning. Multimedia Tools and Applications 80, 1–28. doi:10.1007/s11042-020-09733-5.
- [27] Ershadi-Nasab, S., Noury, E., Kasaei, S., Sanaei, E., 2018. Multiple human 3d pose estimation from multiview images. Multimedia Tools and Applications 77, 15573–15601. URL: <https://doi.org/10.1007/s11042-017-5133-8>, doi:10.1007/s11042-017-5133-8.
- [28] Fan, Z., Li, X., Li, Y., 2021. Multi-agent deep reinforcement learning for online 3d human poses estimation. Remote Sensing 13. URL: <https://www.mdpi.com/2072-4292/13/19/3995>, doi:10.3390/rs13193995.
- [29] Feng, Q., He, K., Wen, H., Keskin, C., Ye, Y., 2023. Rethinking the data annotation process for multi-view 3d pose estimation with active learning and self-training, in: Proceedings of the IEEE/CVF Winter Conference on Applications of Computer Vision (WACV), pp. 5695–5704.
- [30] de França Silva, D.W., do Monte Lima, J.P.S., Macêdo, D., Zanchettin, C., Thomas, D.G.F., Uchiyama, H., Teichrieb, V., 2022. Unsupervised multi-view multi-person 3d pose estimation using reprojection error, in: Artificial Neural Networks and Machine Learning – ICANN 2022, Springer Nature Switzerland, Cham, pp. 482–494.
- [31] de França Silva, D.W., Silva, D. Monte Lima, J.P., Francis Thomas, D.G., Uchiyama, H., Teichrieb, V., 2023.

- Umpose++: Unsupervised multi-view multi-person 3d pose estimation using ground point matching, p. 607 – 614. URL: <https://www.scopus.com/inward/record.uri?eid=2-s2.0-85183599409&doi=10.5220%2F001166880003417&partnerID=40&md5=485a64f86b8058f9915ed28e3324d291>, doi:10.5220/001166880003417.
- [32] Gower, J.C., 1975. Generalized procrustes analysis. *Psychometrika* 40, 33–51. URL: <https://doi.org/10.1007/BF02291478>, doi:10.1007/BF02291478.
- [33] Hassan, M., Eberhardt, J., Malorodov, S., Jäger, M., 2022. Robust multiview 3d pose estimation using time of flight cameras. *IEEE Sensors Journal* 22, 2672–2684. doi:10.1109/JSEN.2021.3133108.
- [34] Holte, M.B., Tran, C., Trivedi, M.M., Moeslund, T.B., 2012. Human pose estimation and activity recognition from multi-view videos: Comparative explorations of recent developments. *IEEE Journal of Selected Topics in Signal Processing* 6, 538–552. doi:10.1109/JSTSP.2012.2196975.
- [35] Huang, C., Jiang, S., Li, Y., Zhang, Z., Traish, J., Deng, C., Ferguson, S., Da Xu, R.Y., 2020. End-to-end dynamic matching network for multi-view multi-person 3d pose estimation, in: *Computer Vision – ECCV 2020*, Springer International Publishing, Cham, pp. 477–493.
- [36] Hwang, T., Kim, J., Kim, M., 2023a. A distributed real-time 3d pose estimation framework based on asynchronous multiviews. *KSII Transactions on Internet and Information Systems* 17, 559–575. doi:10.3837/tiis.2023.02.015.
- [37] Hwang, T., Kim, J., Kim, M., Kim, M., 2023b. A real-time multi-person 3d pose estimation system from multiple rgb-d views for live streaming of 3d animation, in: *Companion Proceedings of the 28th International Conference on Intelligent User Interfaces*, Association for Computing Machinery, New York, NY, USA, p. 105–107. URL: <https://doi.org/10.1145/3581754.3584144>, doi:10.1145/3581754.3584144.
- [38] Insaftudinov, E., Pishchulin, L., Andres, B., Andriluka, M., Schiele, B., 2016. Deepercut: A deeper, stronger, and faster multi-person pose estimation model, in: *Computer Vision – ECCV 2016*, Springer International Publishing, Cham, pp. 34–50.
- [39] Ionescu, C., Papava, D., Olaru, V., Sminchisescu, C., 2014. Human3.6m: Large scale datasets and predictive methods for 3d human sensing in natural environments. *IEEE Transactions on Pattern Analysis and Machine Intelligence* 36, 1325–1339.
- [40] Jenni, S., Favaro, P., 2021. Self-supervised multi-view synchronization learning for 3d pose estimation, in: *Computer Vision – ACCV 2020*, Springer International Publishing, Cham, pp. 170–187.
- [41] Ji, X., Fang, Q., Dong, J., Shuai, Q., Jiang, W., Zhou, X., 2020. A survey on monocular 3d human pose estimation. *Virtual Reality & Intelligent Hardware* 2, 471–500. URL: <https://www.sciencedirect.com/science/article/pii/S2096579620300887>, doi:https://doi.org/10.1016/j.vrih.2020.04.005.
- [42] Jiang, B., Hu, L., Xia, S., 2023. Probabilistic triangulation for uncalibrated multi-view 3d human pose estimation, in: *2023 IEEE/CVF International Conference on Computer Vision (ICCV)*, pp. 14804–14814. doi:10.1109/ICCV51070.2023.01364.
- [43] Joo, H., Simon, T., Li, X., Liu, H., Tan, L., Gui, L., Banerjee, S., Godisart, T.S., Nabbe, B., Matthews, I., Kanade, T., Nobuhara, S., Sheikh, Y., 2017. Panoptic studio: A massively multiview system for social interaction capture. *IEEE Transactions on Pattern Analysis and Machine Intelligence* .
- [44] Kadkhodamohammadi, A., Padoy, N., 2019. A generalizable approach for multi-view 3d human pose regression. *arXiv:1804.10462*.
- [45] Kazemi, V., Burenus, M., Azizpour, H., Sullivan, J., 2013. Multi-view body part recognition with random forests. doi:10.5244/C.27.48.
- [46] Kazemi, V., Sullivan, J., 2012. Using richer models for articulated pose estimation of footballers, in: *BMVC*.
- [47] Kumar, P., Chauhan, S., Awasthi, L.K., 2022. Human pose estimation using deep learning: review, methodologies, progress and future research directions. *International Journal of Multimedia Information Retrieval* 11, 1–33. doi:10.1007/s13735-022-00261-6.
- [48] Kundu, J.N., Seth, S., au2, R.M.V., Rakesh, M., Babu, R.V., Chakraborty, A., 2020. Kinematic-structure-preserved representation for unsupervised 3d human pose estimation. *arXiv:2006.14107*.
- [49] Lan, G., Wu, Y., Hu, F., Hao, Q., 2023. Vision-based human pose estimation via deep learning: A survey. *IEEE Transactions on Human-Machine Systems* 53, 253–268. doi:10.1109/THMS.2022.3219242.
- [50] Lin, J., Lee, G.H., 2021. Multi-view multi-person 3d pose estimation with plane sweep stereo, in: *Proceedings of the IEEE/CVF Conference on Computer Vision and Pattern Recognition (CVPR)*, pp. 11886–11895.
- [51] Lin, J., Li, S., Qin, H., Wang, H., Cui, N., Jiang, Q., Jian, H., Wang, G., 2023. Overview of 3d human pose estimation. *CMES - Computer Modeling in Engineering and Sciences* 134, 1621 – 1651. URL: <https://www.scopus.com/inward/record.uri?eid=2-s2.0-85138834832&doi=10.32604%2Fcmes.2022.020857&partnerID=40&md5=e77e2ad7b0e050ca270f5a2ce7f97d3d>, doi:10.32604/cmes.2022.020857. cited by: 1; All Open Access, Gold Open Access.
- [52] Liu, J., Shahroudy, A., Perez, M., Wang, G., Duan, L.Y., Kot, A.C., 2020. Ntu rgb+d 120: A large-scale benchmark for 3d human activity understanding. *IEEE Transactions on Pattern Analysis and Machine Intelligence* 42, 2684–2701. doi:10.1109/TPAMI.2019.2916873.
- [53] Liu, L., Yang, L., Chen, W., Gao, X., 2021. Dual-view 3d human pose estimation without camera parameters for action recognition. *IET Image Processing* 15, 3433–3440. URL: <https://ietresearch.onlinelibrary.wiley.com/doi/abs/10.1049/ipr2.12277>, doi:https://doi.org/10.1049/ipr2.12277.
- [54] Liu, W., Bao, Q., Sun, Y., Mei, T., 2022. Recent advances of monocular 2d and 3d human pose estimation: A deep learning perspective 55. URL: <https://doi.org/10.1145/3524497>, doi:10.1145/3524497.
- [55] Liu, Z., Zhu, J., Bu, J., Chen, C., 2015. A survey of human pose estimation: The body parts parsing based methods. *Journal of Visual Communication and Image Representation* 32, 10–19. URL: <https://www.sciencedirect.com/science/article/pii/S1047320315001121>, doi:https://doi.org/10.1016/j.jvcir.2015.06.013.
- [56] Ma, Z., Li, K., Li, Y., 2023. Self-supervised method for 3d human pose estimation with consistent shape and viewpoint factorization. *Applied Intelligence* 53, 3864–3876. doi:10.1007/s10489-022-03714-x.
- [57] Manesco, J.R.R., Marana, A.N., 2022. A survey of recent advances on two-step 3d human pose estimation, in: *Xavier-Junior, J.C., Rios, R.A. (Eds.), Intelligent Systems*, Springer International Publishing, Cham, pp. 266–281.
- [58] Mehrizi, R., Peng, X., Tang, Z., Xu, X., Metaxas, D., Li, K., 2018. Toward marker-free 3d pose estimation in lifting: A deep multi-view solution. *arXiv:1802.01741*.
- [59] Mehta, D., Rhodin, H., Casas, D., Fua, P., Sotnychenko, O., Xu, W., Theobalt, C., 2017. Monocular 3d human pose estimation in the wild using improved cnn supervision, in: *3D Vision (3DV), 2017 Fifth International Conference on, IEEE*. URL: http://gvv.mpi-inf.mpg.de/3dhp_dataset, doi:10.1109/3dv.2017.00064.
- [60] Mustafa, A., Russell, C., Hilton, A., 2022. 4d temporally coherent multi-person semantic reconstruction and segmentation. *International Journal of Computer Vision* 130, 1–24. doi:10.1007/s11263-022-01599-4.
- [61] Nakatsuka, C., Komorita, S., 2022. Stable 3d human pose estimation in low-resolution videos with a few views, pp. 427–433. doi:10.1109/ICRA46639.2022.9812382.
- [62] Ohkawa, T., Furuta, R., Sato, Y., 2023. Efficient annotation and learning for 3d hand pose estimation: A survey. *International Journal of Computer Vision* , 1–14doi:10.1007/s11263-023-01856-0.
- [63] Page, M.J., McKenzie, J.E., Bossuyt, P.M.M., Boutron, I., Hoffmann, T.C., Mulrow, C.D., Shamseer, L., Tetzlaff, J.M., Moher, D., 2021. Updating guidance for reporting systematic reviews: development of the prisma 2020 statement. *Journal of clinical epidemiology* .

- [64] Reddy, N., Guigues, L., Pishchulin, L., Eledath, J., Narasimhan, S.G., 2021. Tesseract: End-to-end learnable multi-person articulated 3d pose tracking, in: 2021 IEEE/CVF Conference on Computer Vision and Pattern Recognition (CVPR), IEEE Computer Society, Los Alamitos, CA, USA. pp. 15185–15195. URL: <https://doi.ieeecomputersociety.org/10.1109/CVPR46437.2021.01494>, doi:10.1109/CVPR46437.2021.01494.
- [65] Remelli, E., Han, S., Honari, S., Fua, P., Wang, R., 2020. Lightweight multi-view 3d pose estimation through camera-disentangled representation. arXiv:2004.02186.
- [66] Ren, Y., Wang, Z., Wang, Y., Tan, S., Chen, Y., Yang, J., 2022. Gopose: 3d human pose estimation using wifi. Proceedings of the ACM on Interactive, Mobile, Wearable and Ubiquitous Technologies 6, 1–25. doi:10.1145/3534605.
- [67] Rhodin, H., Salzmann, M., Fua, P., 2018. Unsupervised geometry-aware representation for 3d human pose estimation. arXiv:1804.01110.
- [68] Rochette, G., Russell, C., Bowden, R., 2019. Weakly-supervised 3d pose estimation from a single image using multi-view consistency. arXiv:1909.06119.
- [69] Rohrbach, M., Rohrbach, A., Regneri, M., Amin, S., Andriluka, M., Pinkal, M., Schiele, B., 2015. Recognizing fine-grained and composite activities using hand-centric features and script data. International Journal of Computer Vision, 1–28. URL: <http://dx.doi.org/10.1007/s11263-015-0851-8>, doi:10.1007/s11263-015-0851-8.
- [70] Sarafianos, N., Boteanu, B., Ionescu, B., Kakadiaris, I.A., 2016. 3d human pose estimation: A review of the literature and analysis of covariates. Computer Vision and Image Understanding 152, 1–20. URL: <https://www.sciencedirect.com/science/article/pii/S1077314216301369>, doi:https://doi.org/10.1016/j.cviu.2016.09.002.
- [71] Schwarcz, S., Pollard, T., 2018. 3d human pose estimation from deep multi-view 2d pose, in: 2018 24th International Conference on Pattern Recognition (ICPR), IEEE. URL: <http://dx.doi.org/10.1109/ICPR.2018.8545631>, doi:10.1109/icpr.2018.8545631.
- [72] Shahroudy, A., Liu, J., Ng, T.T., Wang, G., 2016. Ntu rgb+d: A large scale dataset for 3d human activity analysis, in: 2016 IEEE Conference on Computer Vision and Pattern Recognition (CVPR), pp. 1010–1019. doi:10.1109/CVPR.2016.115.
- [73] Shere, M., Kim, H., Hilton, A., 2021. Temporally consistent 3d human pose estimation using dual 360° cameras, in: 2021 IEEE Winter Conference on Applications of Computer Vision (WACV), pp. 81–90. doi:10.1109/WACV48630.2021.00013.
- [74] Sigal, L., Balan, A., Black, M., 2010. Humaneva: Synchronized video and motion capture dataset and baseline algorithm for evaluation of articulated human motion. International Journal of Computer Vision 87, 4–27. doi:10.1007/s11263-009-0273-6.
- [75] Solichah, U., Purnomo, M.H., Yuniarno, E.M., 2020. Markerless motion capture based on openpose model using triangulation, in: 2020 International Seminar on Intelligent Technology and Its Applications (ISITIA), pp. 217–222. doi:10.1109/ISITIA49792.2020.9163662.
- [76] Song, L., Yu, G., Yuan, J., Liu, Z., 2021. Human pose estimation and its application to action recognition: A survey. Journal of Visual Communication and Image Representation 76, 103055. URL: <https://www.sciencedirect.com/science/article/pii/S1047320321000262>, doi:https://doi.org/10.1016/j.jvcir.2021.103055.
- [77] Song, R., Zhang, D., Wu, Z., Yu, C., Xie, C., Yang, S., Hu, Y., Chen, Y., 2022. Rf-url: unsupervised representation learning for rf sensing, in: Proceedings of the 28th Annual International Conference on Mobile Computing And Networking, Association for Computing Machinery, New York, NY, USA. p. 282–295. URL: <https://doi.org/10.1145/3495243.3560529>, doi:10.1145/3495243.3560529.
- [78] Srivastav, V., Issenhuth, T., Kadkhodamohammadi, A., de Mathelin, M., Gangi, A., Padoy, N., 2021. Mvor: A multi-view rgb-d operating room dataset for 2d and 3d human pose estimation. arXiv:1808.08180.
- [79] Tang, Z., Gu, R., Hwang, J.N., 2018. Joint multi-view people tracking and pose estimation for 3d scene reconstruction, in: 2018 IEEE International Conference on Multimedia and Expo (ICME), pp. 1–6. doi:10.1109/ICME.2018.8486576.
- [80] Trumble, M., Gilbert, A., Malleson, C., Hilton, A., Collomosse, J., 2017. Total capture: 3d human pose estimation fusing video and inertial sensors, in: 2017 British Machine Vision Conference (BMVC).
- [81] Tu, H., Wang, C., Zeng, W., 2020. Voxelpose: Towards multi-camera 3d human pose estimation in wild environment. arXiv:2004.06239.
- [82] Wan, X., Chen, Z., Zhao, X., 2023. View consistency aware holistic triangulation for 3d human pose estimation. Computer Vision and Image Understanding 236, 103830. URL: <https://www.sciencedirect.com/science/article/pii/S1077314223002102>, doi:https://doi.org/10.1016/j.cviu.2023.103830.
- [83] Wang, H., Sun, M., 2022. Smart-vposenet: 3d human pose estimation models and methods based on multi-view discriminant network. Knowledge-Based Systems 239, 107992. URL: <https://www.sciencedirect.com/science/article/pii/S0950705121011060>, doi:https://doi.org/10.1016/j.knosys.2021.107992.
- [84] Wang, H., hui Sun, M., Zhang, H., yan Dong, L., 2022. Lhpe-nets: A lightweight 2d and 3d human pose estimation model with well-structural deep networks and multi-view pose sample simplification method. PLoS ONE 17. URL: <https://doi.org/10.1371/journal.pone.0264302>.
- [85] Wang, J., Tan, S., Zhen, X., Xu, S., Zheng, F., He, Z., Shao, L., 2021a. Deep 3d human pose estimation: A review. Computer Vision and Image Understanding 210, 103225. URL: <https://www.sciencedirect.com/science/article/pii/S1077314221000692>, doi:https://doi.org/10.1016/j.cviu.2021.103225.
- [86] Wang, T., Zhang, J., Cai, Y., Yan, S., Feng, J., 2021b. Direct multi-view multi-person 3d pose estimation. arXiv:2111.04076.
- [87] Wang, Y., Guo, L., Lu, Z., Wen, X., Zhou, S., Meng, W., 2021c. From point to space: 3d moving human pose estimation using commodity wifi. IEEE Communications Letters 25, 2235–2239. doi:10.1109/LCOMM.2021.3073271.
- [88] Wang, Z., Chung, R., 2010. Integrating multiple uncalibrated views for human 3d pose estimation, in: Advances in Visual Computing, Springer Berlin Heidelberg, Berlin, Heidelberg. pp. 280–290.
- [89] Xia, H., Zhang, Q., 2022. Vitpose: Multi-view 3d human pose estimation with vision transformer, in: 2022 IEEE 8th International Conference on Computer and Communications (ICCC), pp. 1922–1927. doi:10.1109/ICCC56324.2022.10065997.
- [90] Xie, C., Zhang, D., Wu, Z., Yu, C., Hu, Y., Chen, Y., 2024. Rpm 2.0: Rf-based pose machines for multi-person 3d pose estimation. IEEE Transactions on Circuits and Systems for Video Technology 34, 490–503. doi:10.1109/TCSVT.2023.3287329.
- [91] Xie, C., Zhang, D., Wu, Z., Yu, C., Hu, Y., Sun, Q., Chen, Y., 2023. Rf-based multi-view pose machine for multi-person 3d pose estimation, in: 2023 IEEE International Conference on Multimedia and Expo (ICME), pp. 2669–2674. doi:10.1109/ICME55011.2023.00454.
- [92] Xu, C., Yu, X., Wang, Z., Ou, L., 2020. Multi-view human pose estimation in human-robot interaction, in: IECON 2020 The 46th Annual Conference of the IEEE Industrial Electronics Society, pp. 4769–4775. doi:10.1109/IECON43393.2020.9255211.
- [93] Xu, Y., Kitani, K., 2022. Multi-view multi-person 3d pose estimation with uncalibrated camera networks, in: 33rd British Machine Vision Conference 2022, BMVC 2022, London, UK, November 21–24, 2022, BMVA Press. URL: <https://bmvc2022.mpi-inf.mpg.de/0132.pdf>.
- [94] Ye, H., Zhu, W., Wang, C., Wu, R., Wang, Y., 2022. Faster voxelpose: Real-time 3d human pose estimation by orthographic projection. arXiv:2207.10955.
- [95] Yin, W., Chen, L., Huang, X., Huang, C., Wang, Z., Bian, Y., Wan, Y., Zhou, Y., Han, T., Yi, M., 2024. A self-supervised spatio-temporal attention network for video-based 3d infant pose estimation. Medical Image Analysis 96,

103208. URL: <https://www.sciencedirect.com/science/article/pii/S1361841524001336>, doi:<https://doi.org/10.1016/j.media.2024.103208>.
- [96] Zhang, D., Wu, Y., Guo, M., Chen, Y., 2021a. Deep learning methods for 3d human pose estimation under different supervision paradigms: A survey. *Electronics* 10. URL: <https://www.mdpi.com/2079-9292/10/18/2267>, doi:10.3390/electronics10182267.
- [97] Zhang, X., Wang, M., Zeng, M., Kang, W., Deng, F., 2023. Humomm: A multi-modal dataset and benchmark for human motion analysis, in: Lu, H., Ouyang, W., Huang, H., Lu, J., Liu, R., Dong, J., Xu, M. (Eds.), *Image and Graphics*, Springer Nature Switzerland, Cham, pp. 204–215. doi:10.1007/978-3-031-46305-1_17.
- [98] Zhang, Y., Wang, C., Wang, X., Liu, W., Zeng, W., 2021b. Voxel-track: Multi-person 3d human pose estimation and tracking in the wild. arXiv:2108.02452.
- [99] Zhao, J., Yu, T., An, L., Huang, Y., Deng, F., Dai, Q., 2024. Triangulation residual loss for data-efficient 3d pose estimation, in: *Proceedings of the 37th International Conference on Neural Information Processing Systems*, Curran Associates Inc., Red Hook, NY, USA.
- [100] Zheng, C., Wu, W., Chen, C., Yang, T., Zhu, S., Shen, J., Ketharnavaz, N., Shah, M., 2023. Deep learning-based human pose estimation: A survey. *ACM Comput. Surv.* URL: <https://doi.org/10.1145/3603618>, doi:10.1145/3603618. just Accepted.
- [101] Zhou, M., Liu, R., Yi, P., Zhou, D., Zhang, Q., Wei, X., 2022. Er-net: Efficient recalibration network for multi-view multi-person 3d pose estimation, in: *2022 8th International Conference on Virtual Reality (ICVR)*, pp. 298–305. doi:10.1109/ICVR55215.2022.9847965.
- [102] Zhu, A., Snoussi, H., Cherouat, A., 2014. Articulated human motion tracking with foreground learning, in: *2014 22nd European Signal Processing Conference (EUSIPCO)*, pp. 366–370.
- [103] Zhu, Z., Liu, S., Shuai, J., Du, S., Li, Y., 2023. 3d associative embedding: Multi-view 3d human pose estimation in crowded scenes, in: *Proceedings of the 2023 4th International Conference on Computing, Networks and Internet of Things*, Association for Computing Machinery, New York, NY, USA. p. 131–139. URL: <https://doi.org/10.1145/3603781.3603804>, doi:10.1145/3603781.3603804.
- [104] Zhuang, Z., Zhou, Y., 2023. Fastervoxelpose+: Fast and accurate voxel-based 3d human pose estimation by depth-wise projection decay, p. 1763 – 1778. URL: <https://www.scopus.com/inward/record.uri?eid=2-s2.0-85189627610&partnerID=40&md5=159b2ac1f0e5a5b11c23b439bb0410c2>.